

# Elliptic flow splitting between protons and antiprotons from hadronic potentials

Pengcheng Li (李鹏程)



Collaborators: Qingfeng Li (HUZU), Yongjia Wang (HUZU),  
Jan Steinheimer (FIAS), Hongfei Zhang (LZU)



- 1 / Background
  - 2 / UrQMD model
  - 3 / Results and discussions
  - 4 / Summary and outlook
-

1 / Background

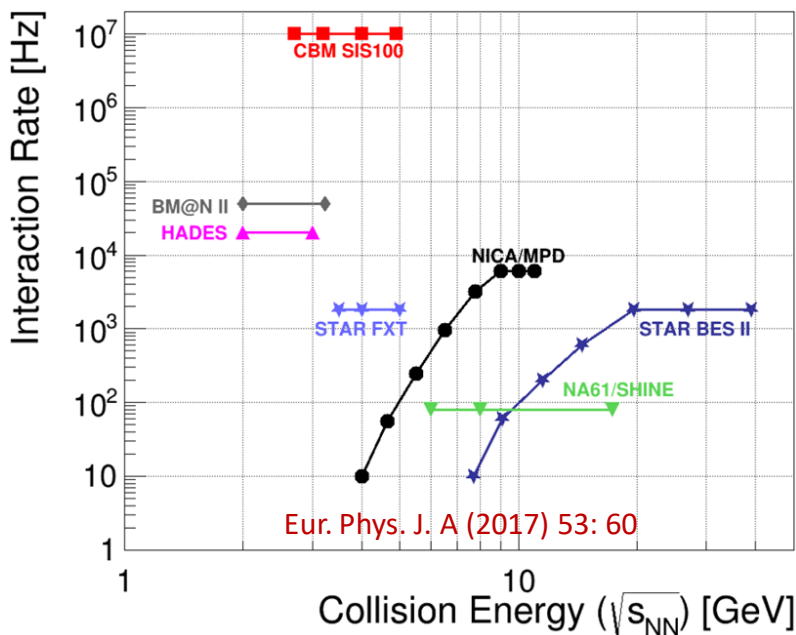
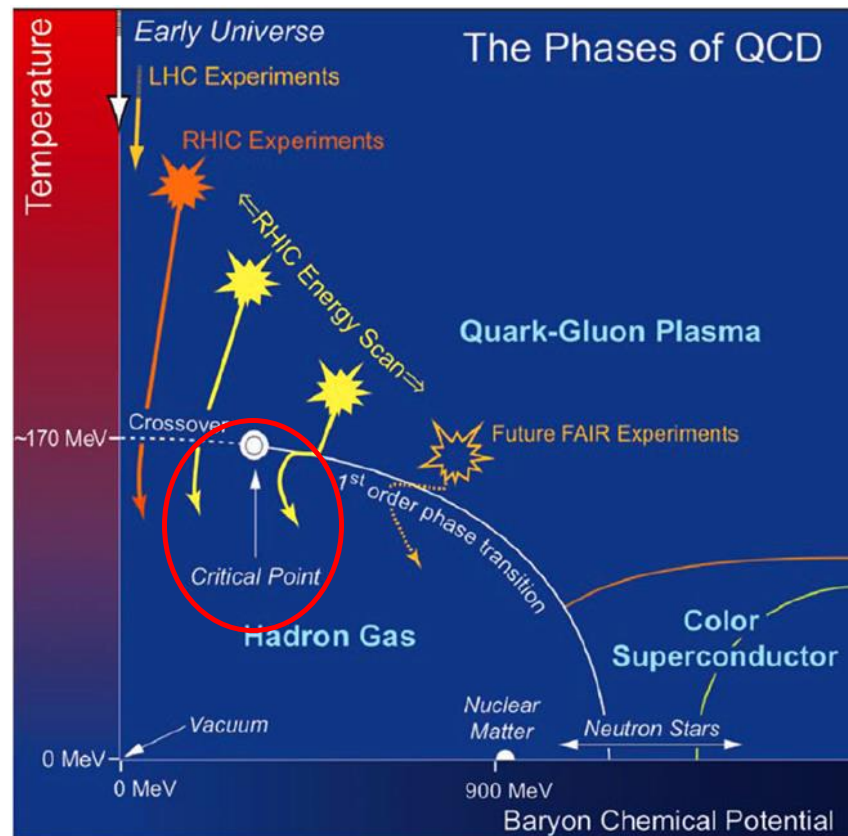
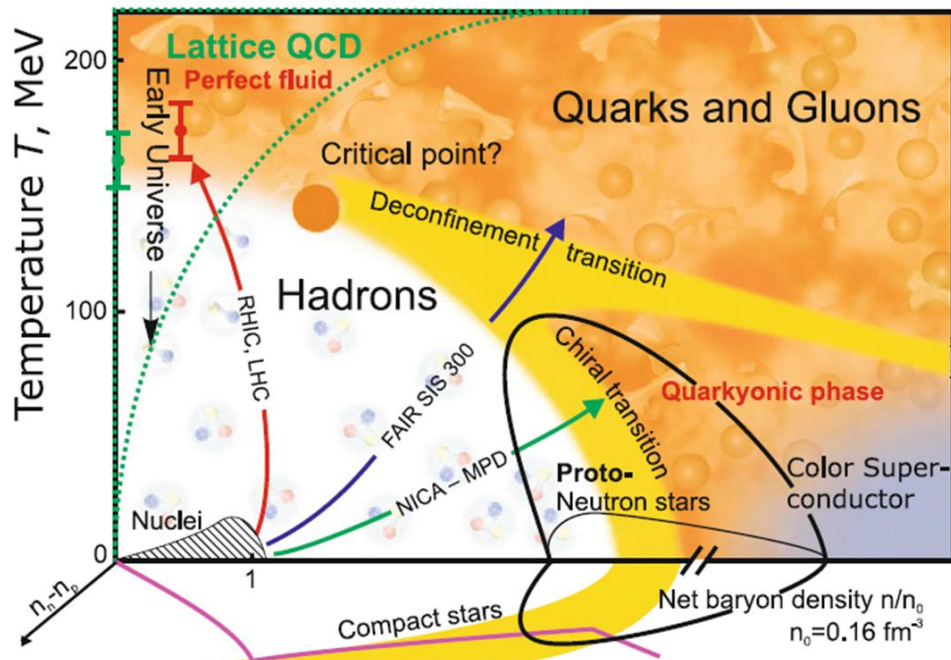
2 / UrQMD model

3 / Results and discussions

4 / Summary and outlook

---

# Background

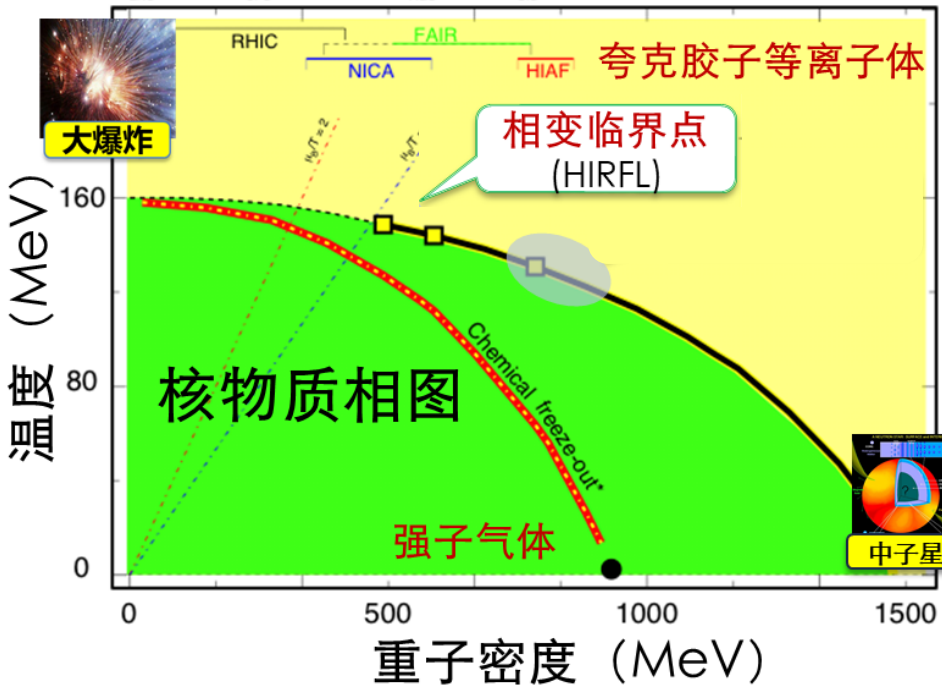


- Search for the **critical point** and the first order phase boundary.
- Study the properties of the QGP.

CBM at FAIR:  $\sqrt{s_{NN}} = 2.7 - 4.9 \text{ GeV}$

NICA:  $\sqrt{s_{NN}} = 4 - 11 \text{ GeV}$

STAR-BES II:  $\sqrt{s_{NN}} = 7.7 - 19.6 \text{ GeV}$



## 1) 基于HIRFL研究高重子密度区核物质相结构

- 研究目标：  
高重子密度区核物质相结构和**临界点**

## 2) 核物质拓扑性质的研究

- 研究目标：  
强相互作用核物质的**拓扑性质**和在**极限外场**(极限角动量、极限强磁场)下的**行为、QCD临界点**

---From RIBLL 2019, Xiaohong Zhou

Table 1 Typical beam parameters from the BRing. The beam intensities are given in the unit of particles per pulse (ppp).

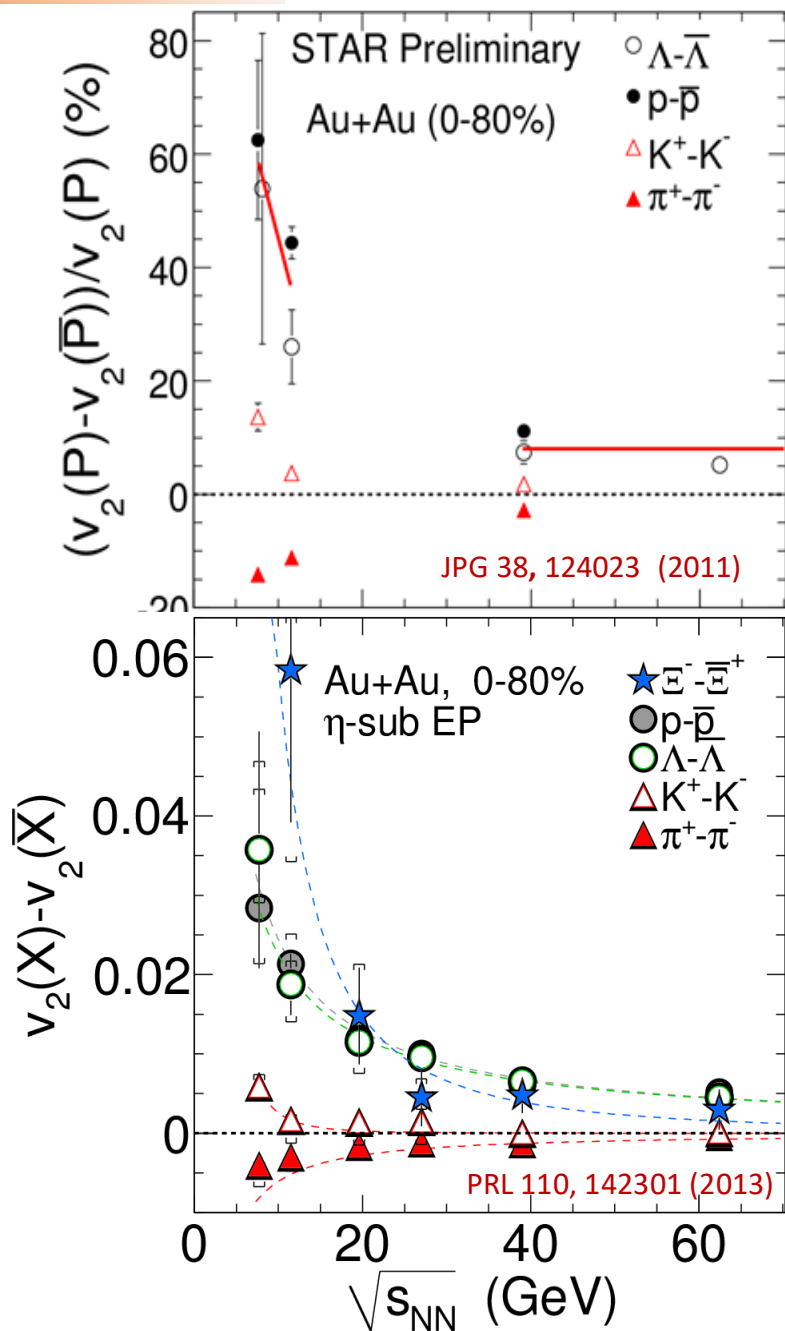
Ion species	Energy/(GeV/u)	Intensity/ppp
P	9.30	$2.0 \times 10^{12}$
$^{18}\text{O}^{6+}$	2.60	$6.0 \times 10^{11}$
$^{78}\text{Kr}^{19+}$	1.70	$3.0 \times 10^{11}$
$^{209}\text{Bi}^{31+}$	0.85	$1.2 \times 10^{11}$
$^{238}\text{U}^{34+}$	0.80	$1.0 \times 10^{11}$

### SRing

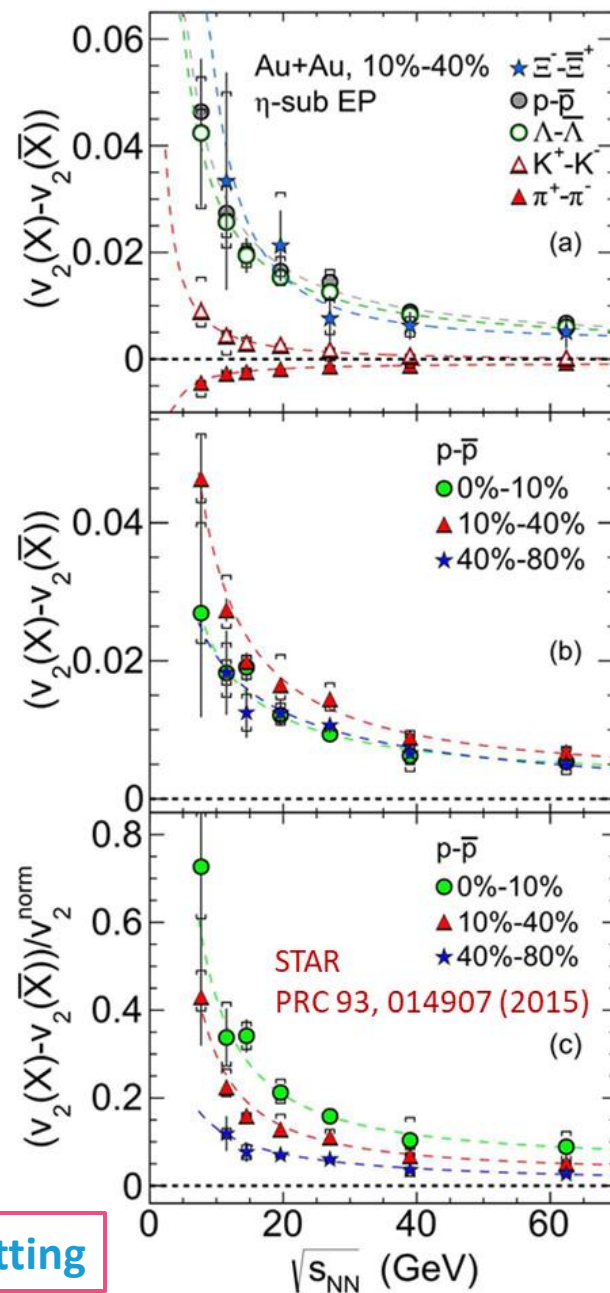
最大磁刚度 15 Tm       $1.0 \times 10^7$  ppp(放射性次级束流)  
 1.5 GeV/u ( $A/Z = 2$ )       $10^9 \sim 10^{10}$  ppp(高电荷态稳定重离子束)  
 1.0 GeV/u ( $^{238}\text{U}^{92+}$ )

Guoqing Xiao, *et al.*, Nuclear Physics Review, 2017, 34(3): 275-283.  
 Xiaohong Zhou, Nuclear Physics Review, 2018, 35(4): 339-349.

# Highlights of recent RHIC physics



$v_2$  splitting



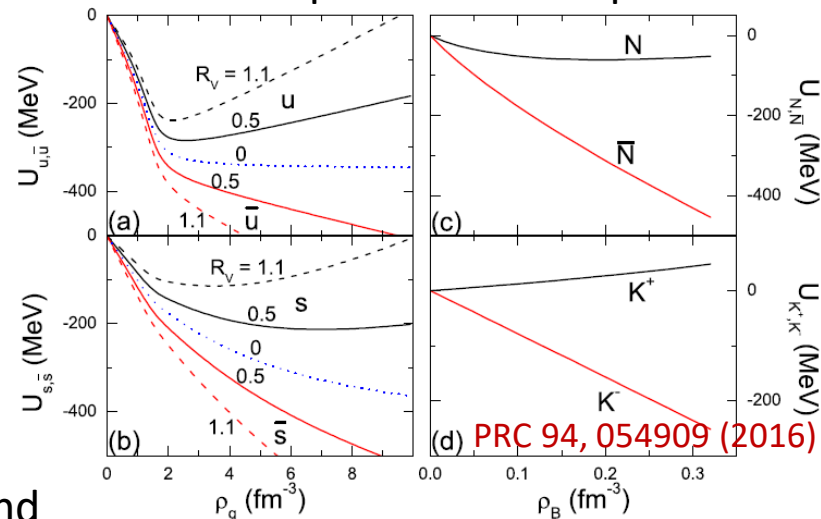
Different hadronic and partonic potentials for particles and antiparticles

J. Xu, L.W. Chen, C.M. Ko, Z.W. Lin, PRC 85, 041901(R) (2012); J. Xu, T. Song, C. M. Ko, F. Li, PRL 112, 012301 (2014)

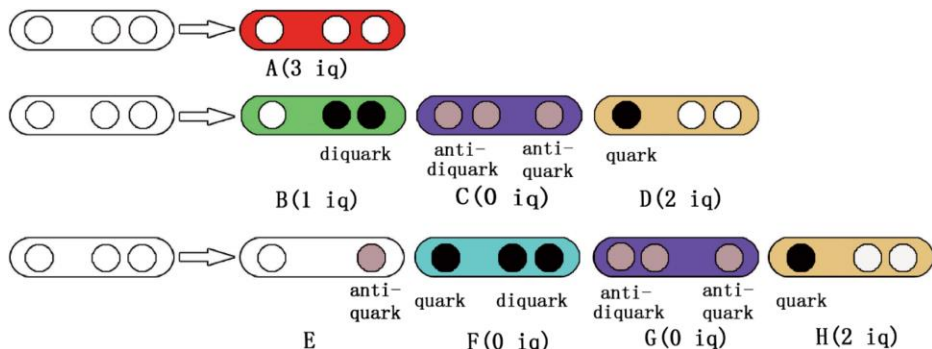
the different mean-field potentials for hadrons and antihadrons or quarks and antiquarks:

- Stronger **attractive** potential for  $\bar{p}$  compared to  $p$   
 → smaller  $v_2(p)$ ,
- **Attractive** potential for  $K^-$ , **repulsive** for  $K^+$   
 →  $v_2(K^-) < v_2(K^+)$ ,
- Slightly **attractive** potential for  $\pi^+$ , **repulsive** for  $\pi^-$   
 →  $v_2(\pi^+) < v_2(\pi^-)$ .

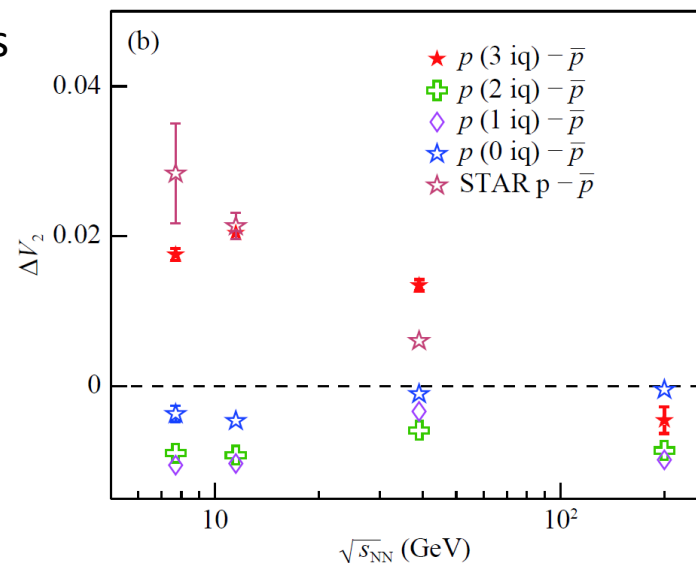
A **repulsive** vector mean-field potential for **quarks** but an **attractive** one for **antiquarks** in a baryon-rich quark matter.



The difference of  $v_2$  between transported quarks and produced quarks. (By tracing the number of initial quarks in protons) B. Tu, et al., CPC 43, 054106 (2019).



Y. Gao, et al., PRC 86, 044901 (2012).



1 / Background

2 / UrQMD model

3 / Results and discussions

4 / Summary and outlook

---



- Baryons are represented by Gaussian wave packets in the phase

$$\phi_i(\mathbf{r}, t) = \frac{1}{(2\pi L)^{3/4}} \exp\left(-\frac{(\mathbf{r} - \mathbf{r}_i)^2}{4L}\right) \exp\left(\frac{i\mathbf{p}_i \cdot \mathbf{r}}{\hbar}\right)$$

- The Wigner distribution function  $f_i$  of the baryon  $i$

$$f_i(\mathbf{r}, \mathbf{p}) = \frac{1}{(\pi\hbar)^3} \exp\left(-\frac{(\mathbf{r} - \mathbf{r}_i)^2}{2L}\right) \exp\left(-\frac{(\mathbf{p} - \mathbf{p}_i)^2 \cdot 2L}{\hbar^2}\right)$$

- Propagated according to Hamilton's equation of motion

$$H = T + U$$

$$\dot{\mathbf{r}}_i = \frac{\partial H}{\partial \mathbf{p}_i} \quad \text{and} \quad \dot{\mathbf{p}}_i = -\frac{\partial H}{\partial \mathbf{r}_i} \quad T = \sum_i (E_i - m_i) = \sum_i (\sqrt{m_i^2 + \mathbf{p}_i^2} - m_i)$$

$$U = U_{\text{Sky}}^2 + U_{\text{Sky}}^3 + U_{\text{Yuk}} + U_{\text{Cou}} + U_{\text{Pau}}$$

- The Skyrme potential

$$U = \alpha \left(\frac{\rho_b}{\rho_0}\right) + \beta \left(\frac{\rho_b}{\rho_0}\right)^\gamma \quad \alpha, \beta, \gamma \rightarrow \text{stiffness of the EoS}$$

Charged particles    SIS energies

- The density of the baryon

$$\rho_b = \int \rho(\mathbf{r}_i) \rho d\mathbf{r} = \int \rho(\mathbf{r}_i) \sum_j \rho(\mathbf{r}_j) d\mathbf{r} = \frac{1}{(4\pi L^2)^{3/2}} \sum_j e^{-\frac{(\mathbf{r}_i - \mathbf{r}_j)^2}{4L^2}}$$

## Potential updates

- The momentum-dependent term:  $U_{md} = \sum_{k=1,2} \frac{t_{md}^k}{\rho_0} \int d\mathbf{p}_j \frac{f(\mathbf{r}_i, \mathbf{p}_j)}{1 + [(\mathbf{p}_i - \mathbf{p}_j)/a_{md}^k]^2}$
- Hamiltonian: the sum of the single-particle energy  $E_i$

$$H = \sum_{i=1}^N \sqrt{\mathbf{p}_i^2 + m_i^2 + 2m_i V_i},$$

The equations of motion are then:

$$\frac{d\mathbf{r}_i}{dt} \approx \frac{\partial H}{\partial \mathbf{p}_i} = \frac{\mathbf{p}_i}{E_i} + \sum_{j=1}^N \frac{m_j}{E_i} \frac{\partial V_i}{\partial \mathbf{p}_i},$$

$$\frac{d\mathbf{p}_i}{dt} \approx -\frac{\partial H}{\partial \mathbf{r}_i} = -\sum_{j=1}^N \frac{m_j}{E_i} \frac{\partial V_i}{\partial \mathbf{r}_i}.$$

The relativistic effects on the relative distance and the relative momentum:

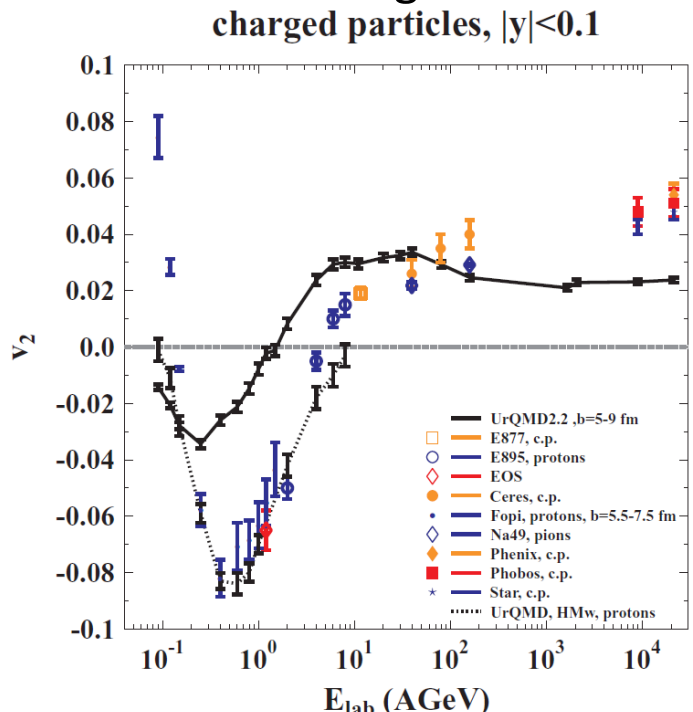
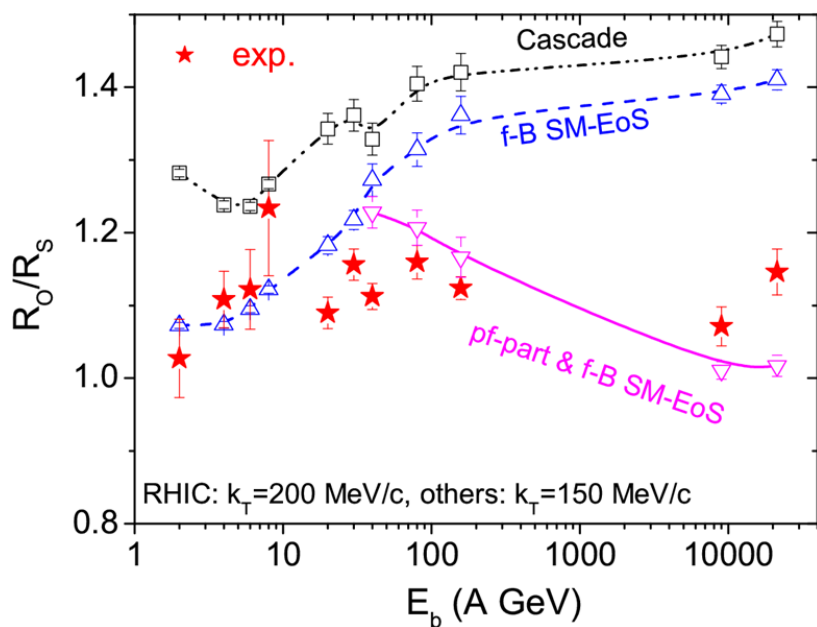
$$\tilde{\mathbf{r}}_{ij}^2 = \mathbf{r}_{ij}^2 + \gamma_{ij}^2 (\mathbf{r}_{ij} \cdot \boldsymbol{\beta}_{ij})^2,$$

$$\tilde{\mathbf{p}}_{ij}^2 = \mathbf{p}_{ij}^2 - (E_i - E_j)^2 + \gamma_{ij}^2 \left( \frac{m_i^2 + m_j^2}{E_i + E_j} \right),$$

$$\boldsymbol{\beta}_{ij} = \frac{\mathbf{p}_i + \mathbf{p}_j}{E_i + E_j}, \quad \gamma_{ij} = \frac{1}{1 - \beta_{ij}^2}.$$

# Potential updates

- At higher beam energies, the Yukawa-, Pauli-, and symmetry-potentials of baryons becomes negligible, while the Skyrme- and the momentum-dependent part of potentials still influence the whole dynamical process of HICs
- Potentials for pre-formed hadrons
  - At high energies, particle production is dominated by the string mechanism
  - The formation time of the hadron is determined by the “yo-yo” mode. During this time, the **pre-formed particles (string fragments that will be projected onto hadron states later)** are usually treated to be free-streaming.



## How to consider the potential for “pre-formed” hadrons?

A



For “pre-formed” particles from string fragmentation, the similar density dependent terms as the formed baryons are used, but without the Yukawa, the Coulomb, and the momentum dependent terms.

B



The “pre-formed” mesons act like “pre-formed” baryons but with a reduction factor (2/3) due to the quark-number difference.

C



The potential interaction between formed and “pre-formed” particles is neglected.

D



The “pre-formed” particles also contribute to the hadronic density (for “pre-formed” mesons, the 2/3 factor is considered).

$$U = \mu \left( \frac{\rho_h}{\rho_0} \right) + \nu \left( \frac{\rho_h}{\rho_0} \right)^g, \quad \rho_h = \sum_{i \neq j} c_i c_j \rho_{ij}$$

$c_{i,j} = 1$ : formed and pre-formed baryons,

$c_{i,j} = 2/3$ : pre-formed mesons;

$c_{i,j} = 0$ : formed mesons

1 / Background

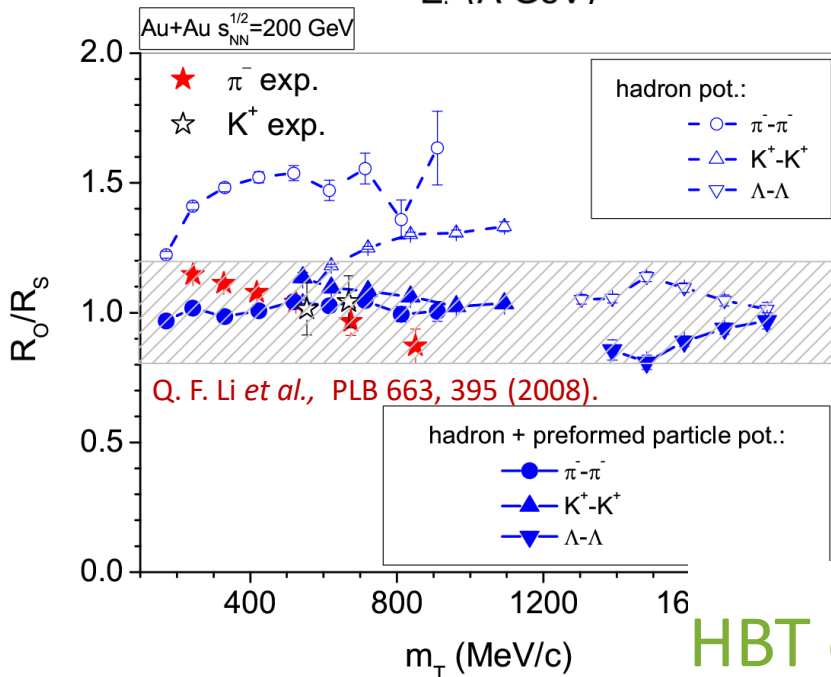
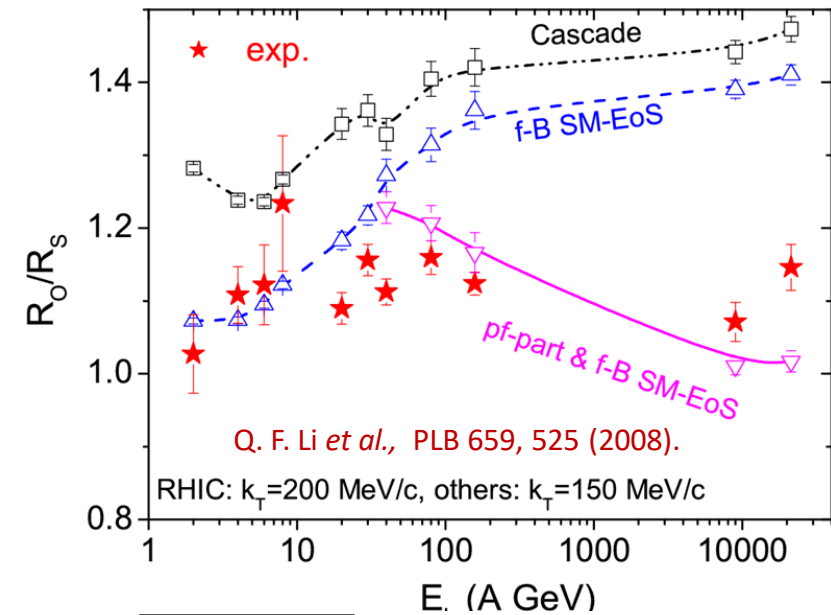
2 / UrQMD model

3 / Results and discussions

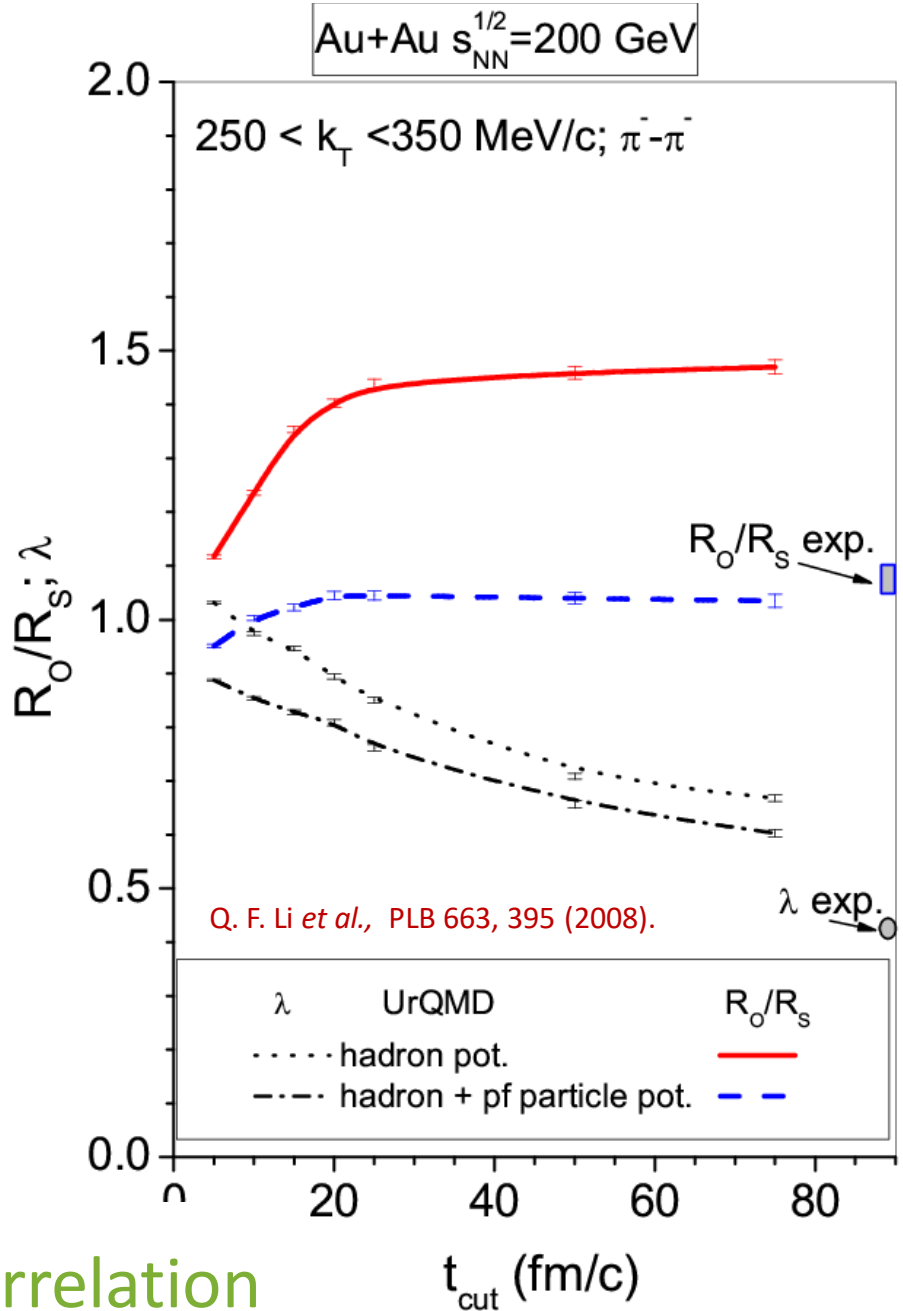
4 / Summary and outlook

---

# Results and discussions



HBT correlation



# Results and discussions

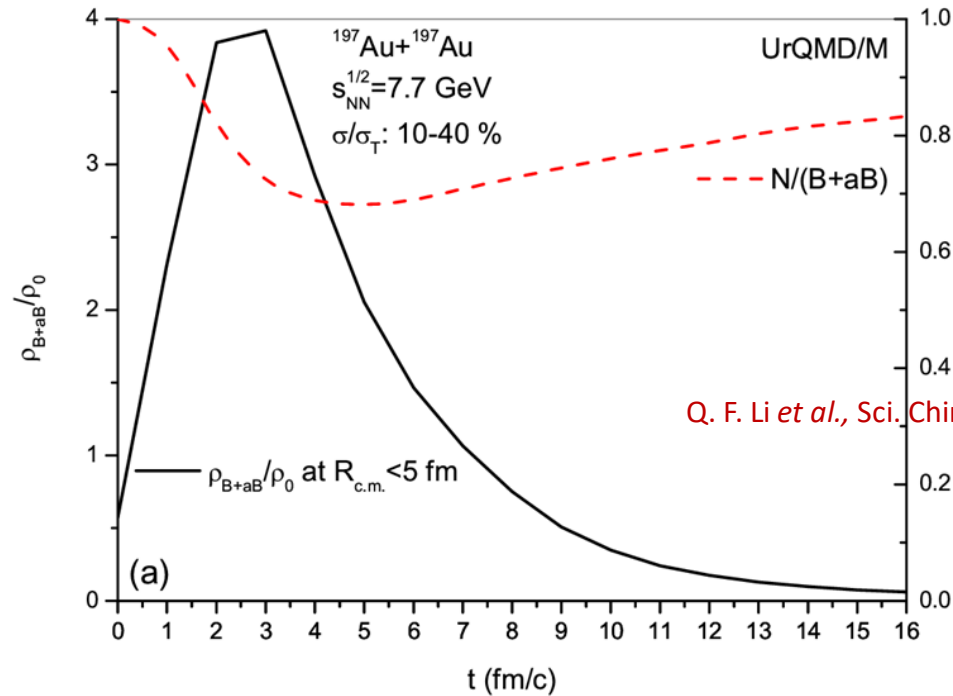
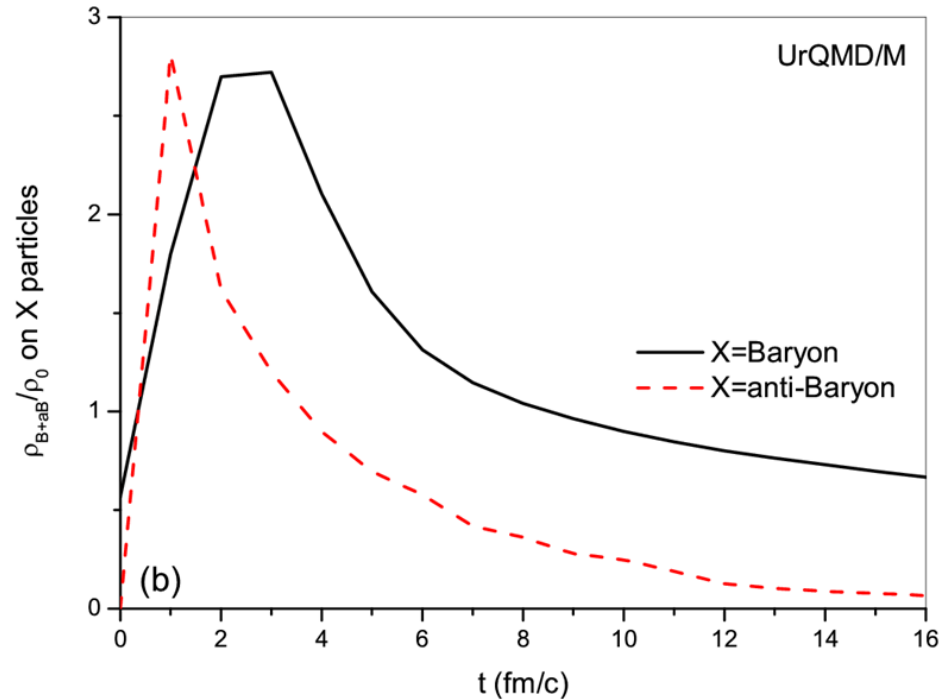
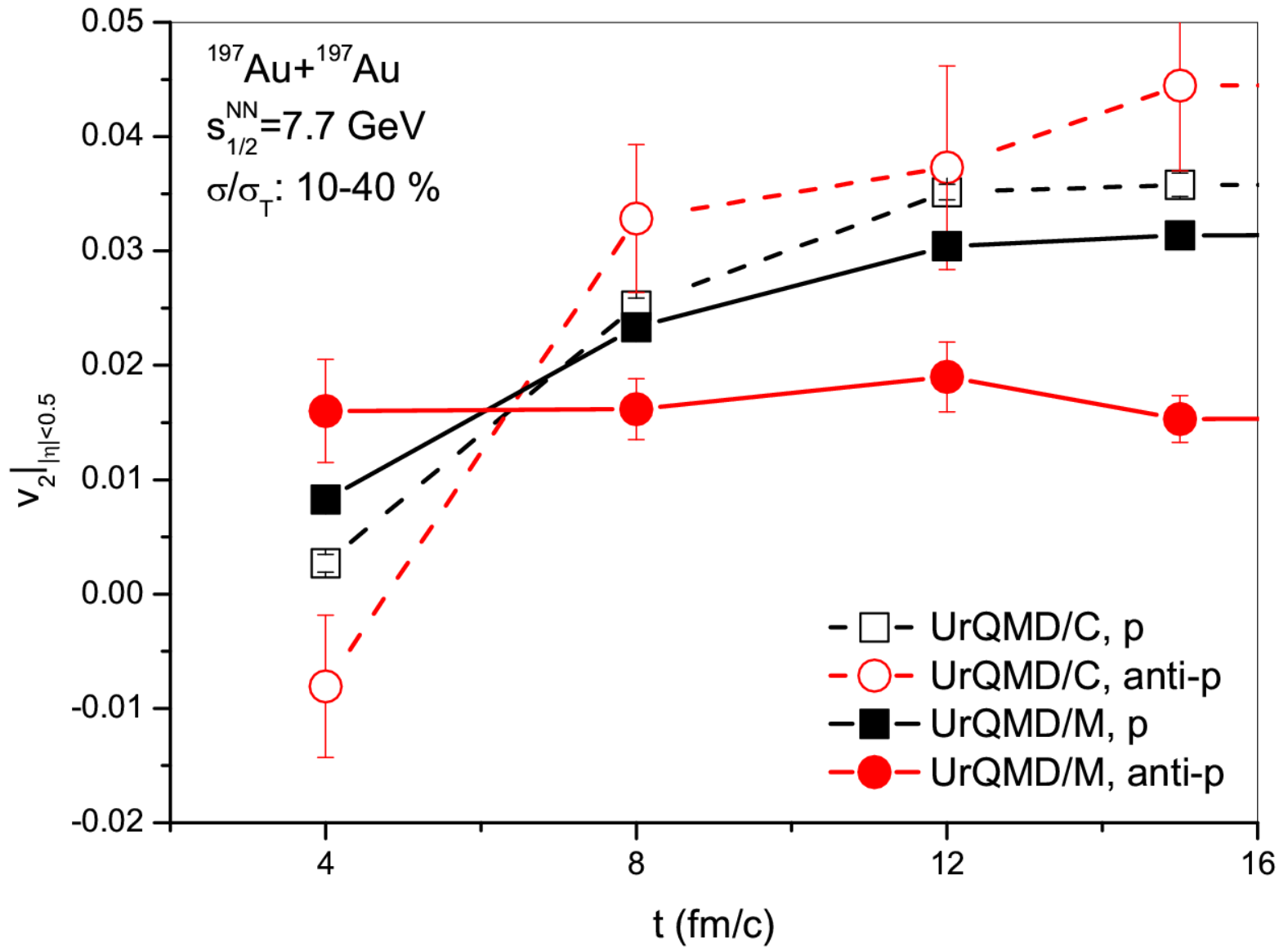


Fig.(a), the maximum value of  $\rho_{B+\bar{B}}/\rho_0$  happens as early as  $\sim 3$  fm/c, and returns to normal density at about  $7\sim 8$  fm/c.

Q. F. Li *et al.*, *Sci. China Phys. Mech. Astron.* 59, 632001 (2016).

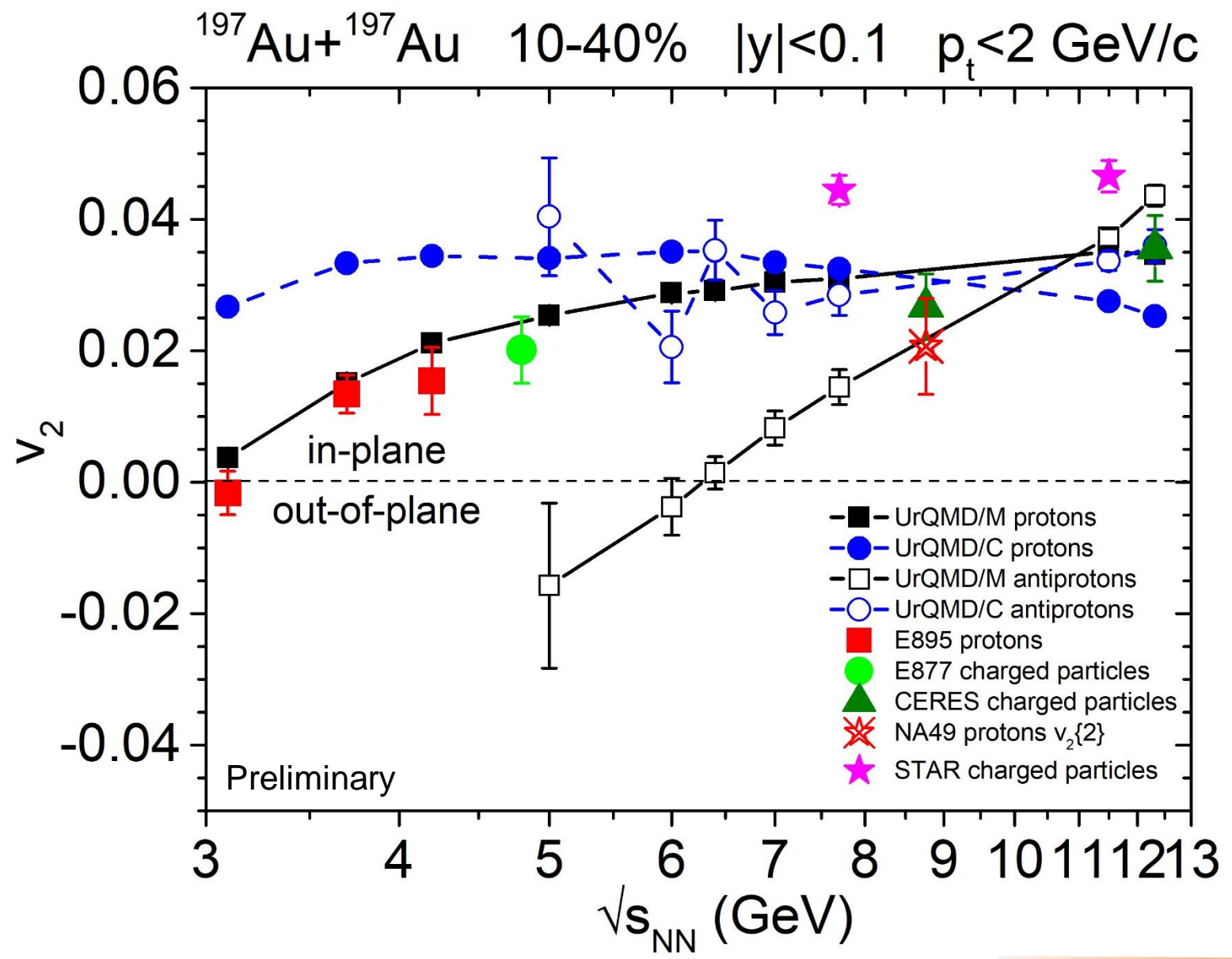
Fig.(b), the (pre-formed) anti-baryons are produced at even earlier times  $\sim 1$ fm/c, and frozen out faster than baryons, since at about 4 fm/c the reduced density has already turned back to the normal one.





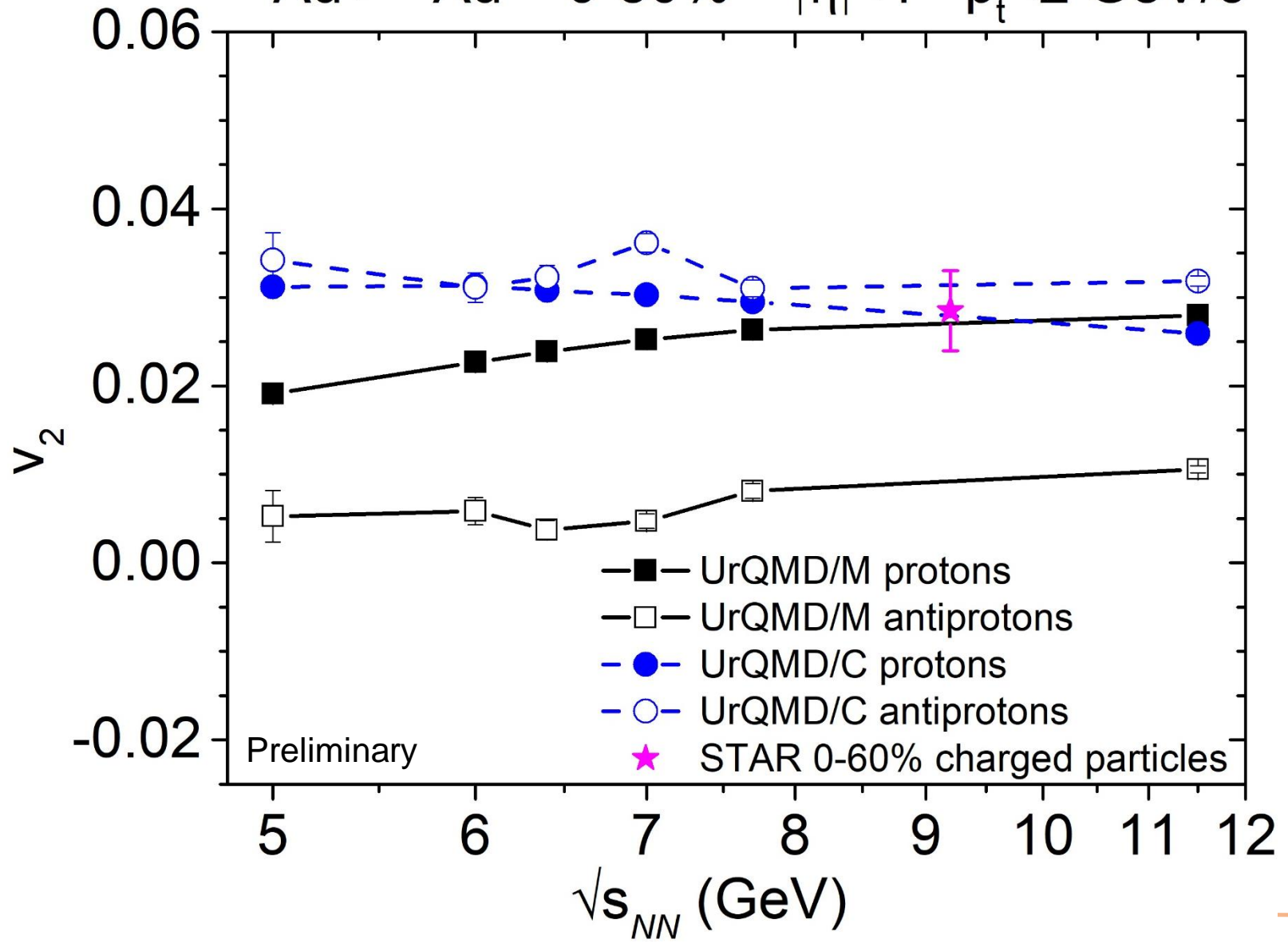
Effects of hadronic mean-field potentials on  $v_2$  splitting





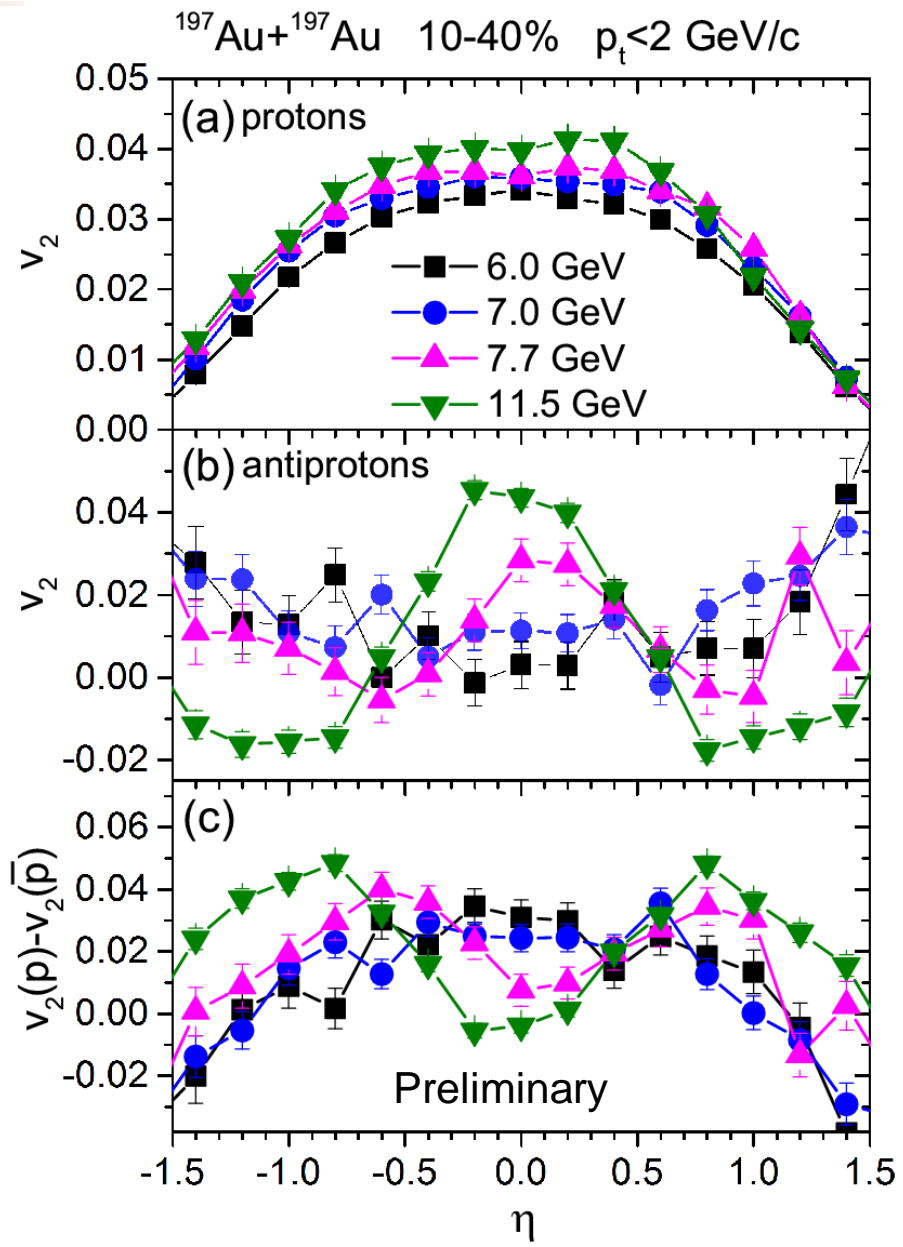
Effects of hadronic mean-field potentials on  $v_2$  splitting

$^{197}\text{Au} + ^{197}\text{Au}$  0-80%  $|\eta| < 1$   $p_t < 2$  GeV/c



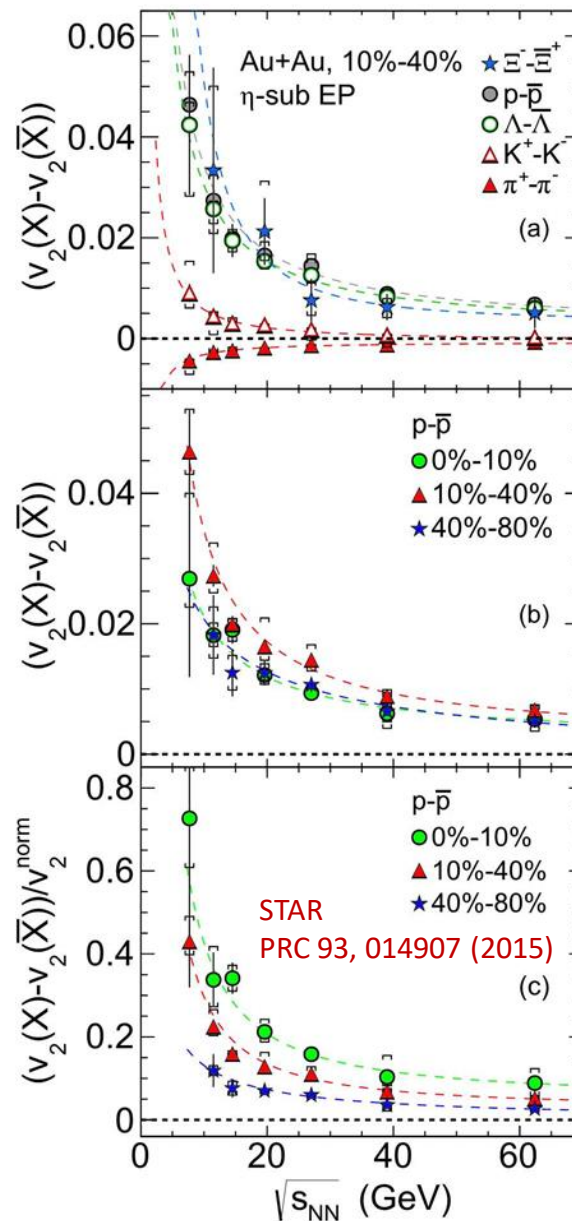
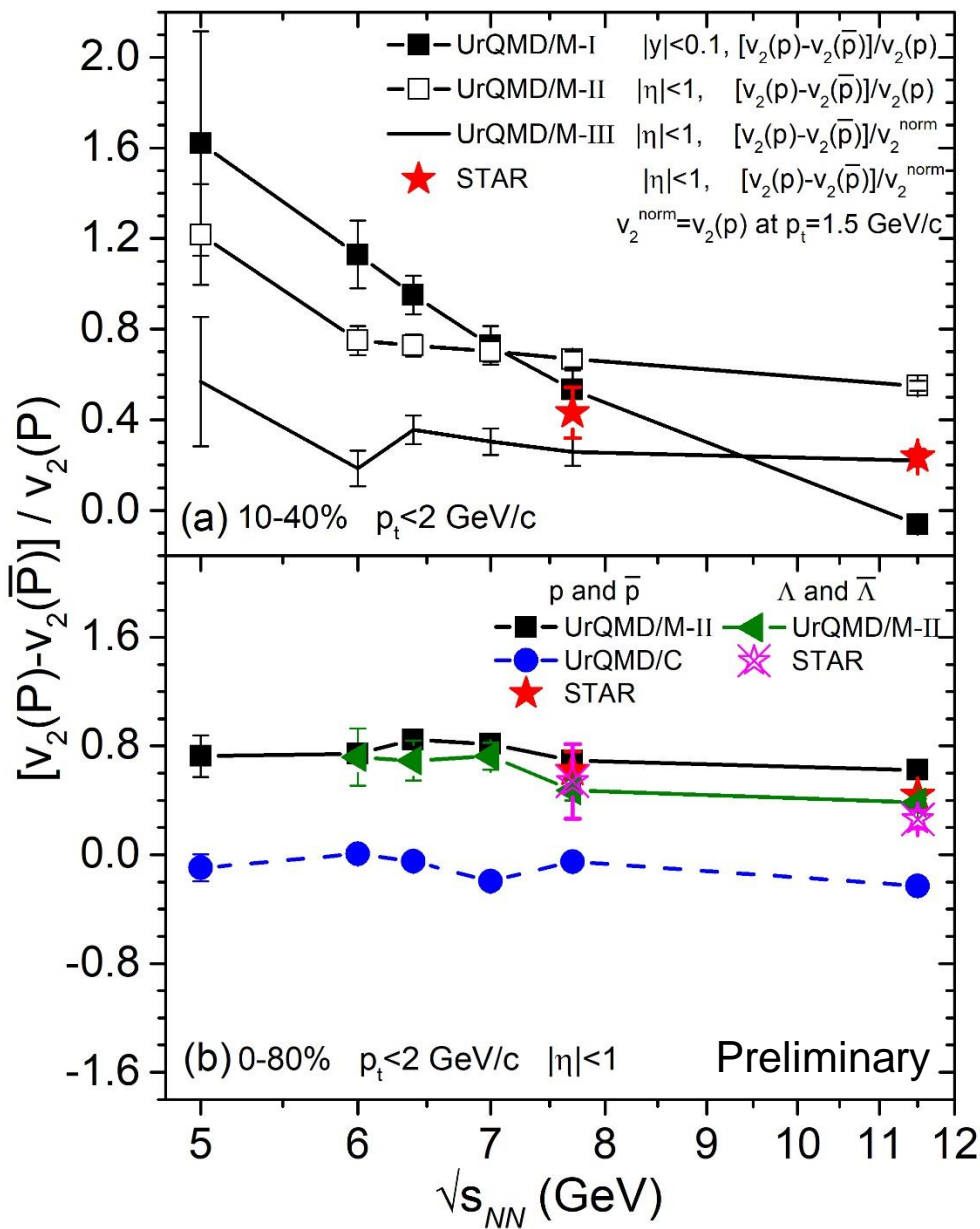
Effects of hadronic mean-field potentials on  $v_2$  splitting

# Results from UrQMD: $v_2$ difference



Effects of hadronic mean-field potentials on  $v_2$  splitting

# Results from UrQMD: $v_2$ difference



Effects of hadronic mean-field potentials on  $v_2$  splitting

- 1 / Background
  - 2 / UrQMD model
  - 3 / Results and discussions
  - 4 / Summary and outlook
-



The  $v_2$  splitting, observed for particles and antiparticles, can be explained by the inclusion of proper hadronic interactions.



The difference in  $v_2$  between protons and antiprotons depends on the centrality and the rapidity windows. With smaller centrality and/or rapidity acceptance, the observed  $v_2$  splitting is more sensitive to the beam energy, indicating a stronger net baryon density dependence of the effect.



The  $v_2$  splitting for 0-80% central Au+Au collisions with  $|\eta| < 1$  still exists below 7.7 GeV, and the splitting does not strongly depend on the collision energy.



We therefore suggest to measure the difference of  $v_2$  between protons and antiprotons at various centralities and rapidity bins at lower beam energies as an indicator to explore the nuclear potential in this beam energy range.

# THANKS

Pengcheng Li | [lipch16@lzu.edu.cn](mailto:lipch16@lzu.edu.cn)

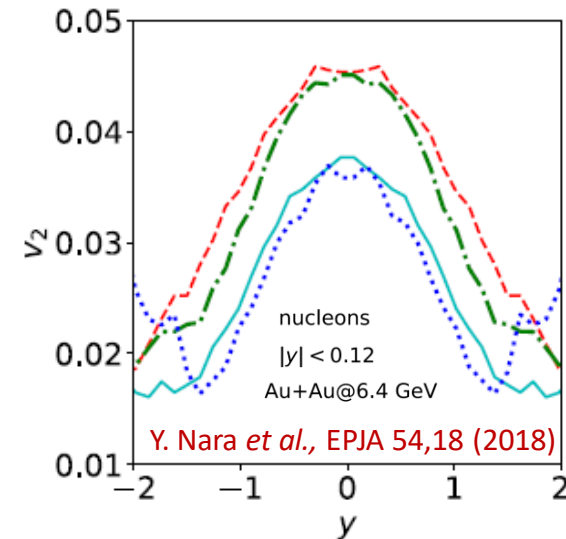
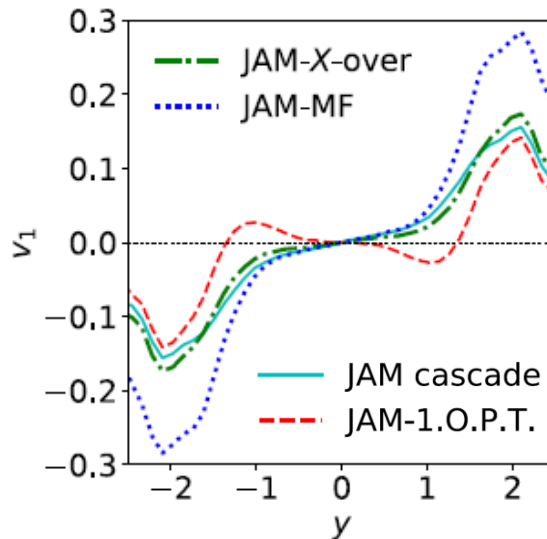
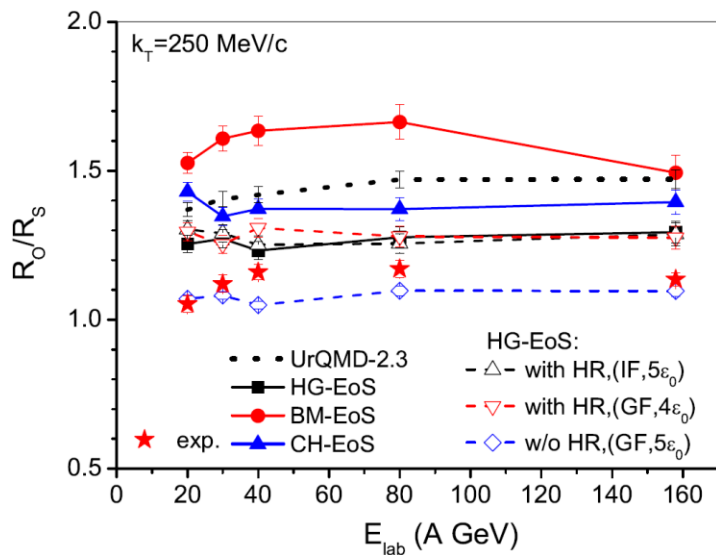
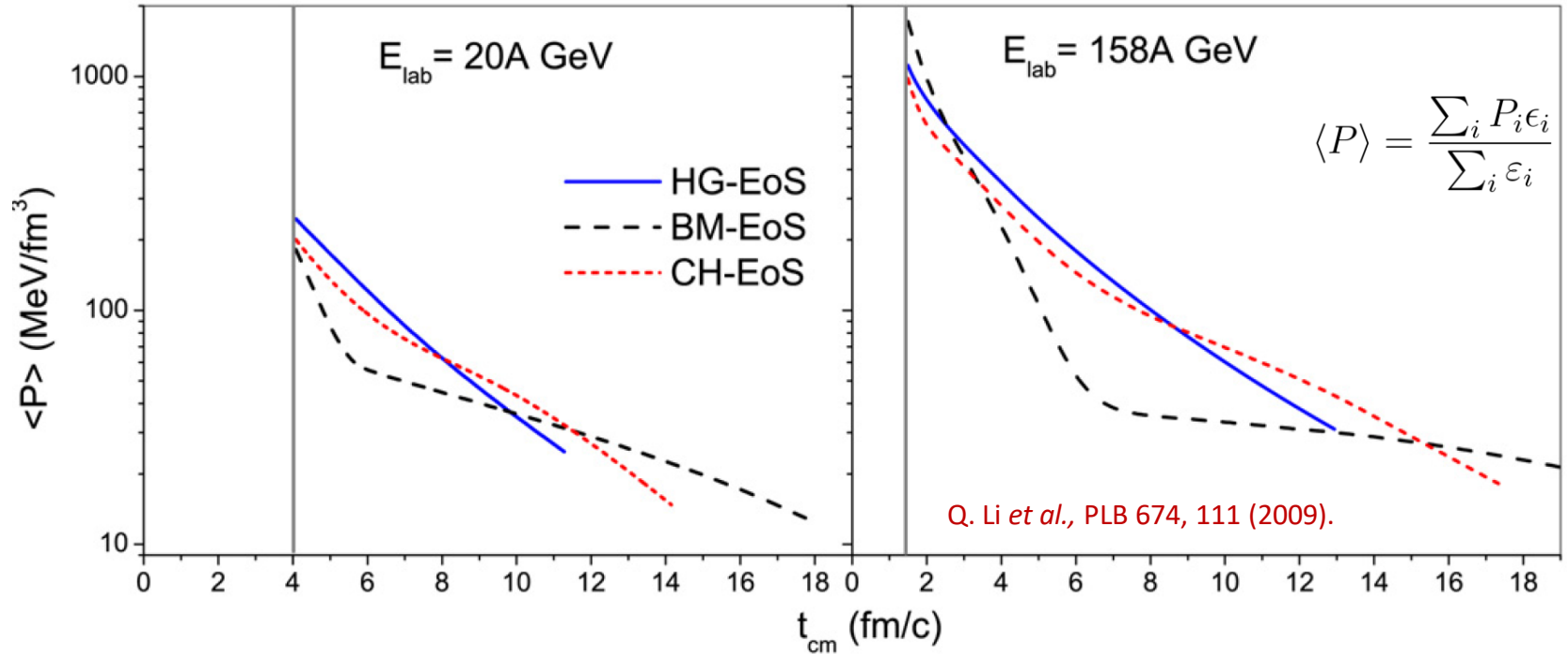
Qingfeng Li | [liqf@zjhu.edu.cn](mailto:liqf@zjhu.edu.cn)

---

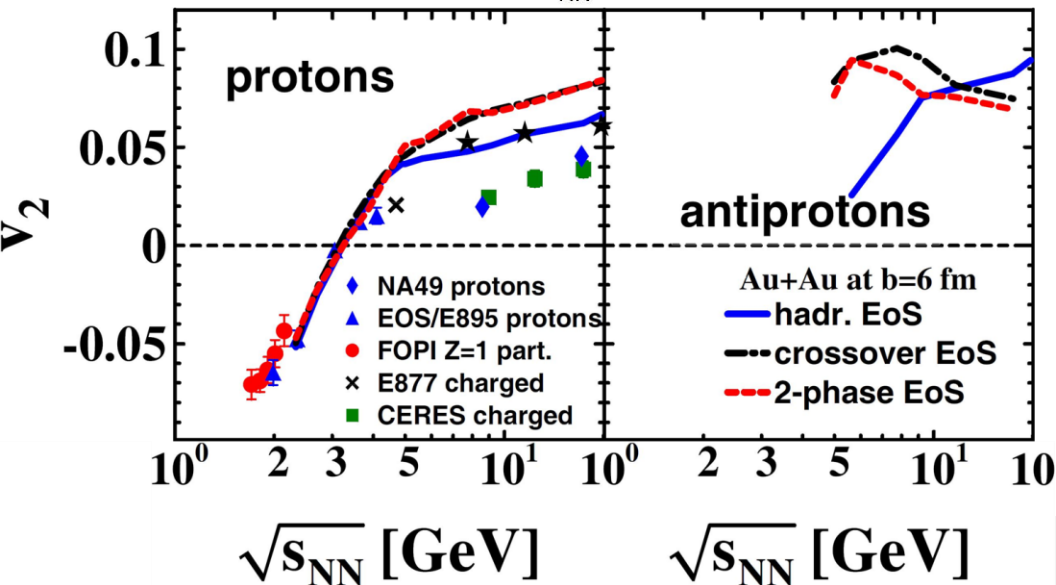
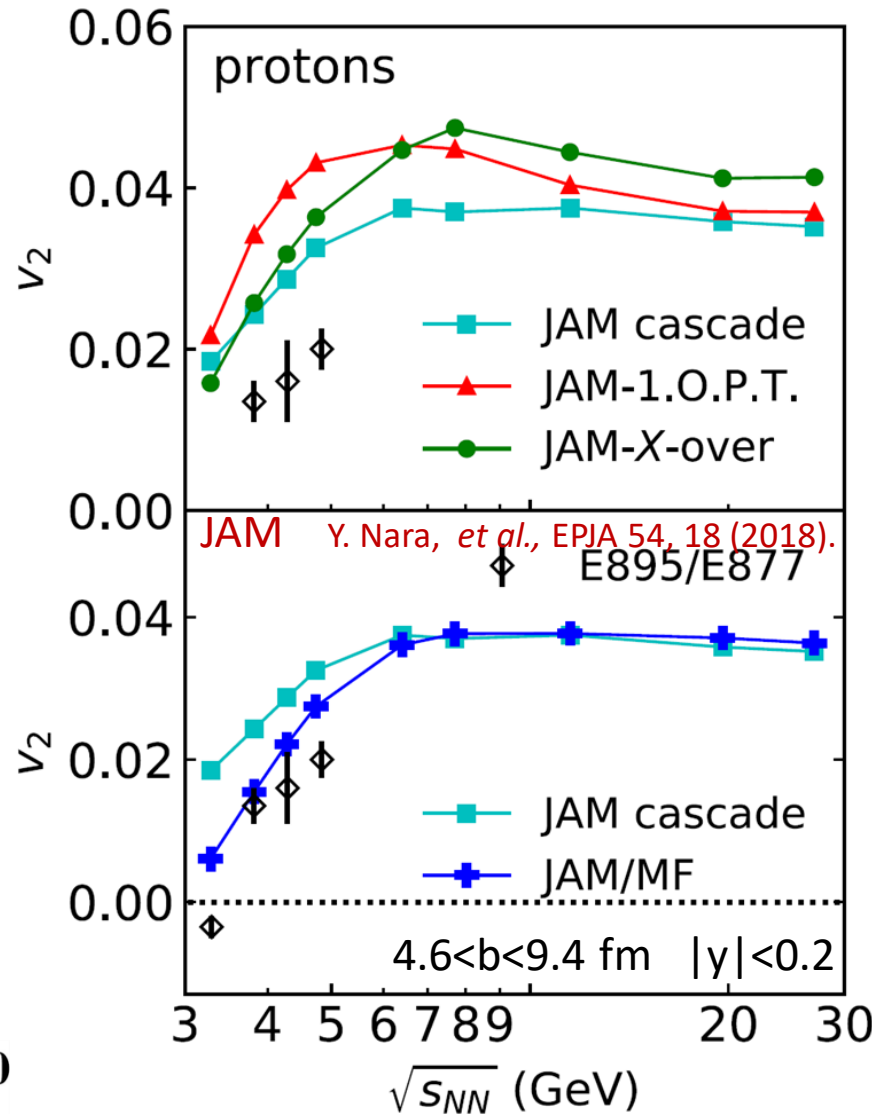
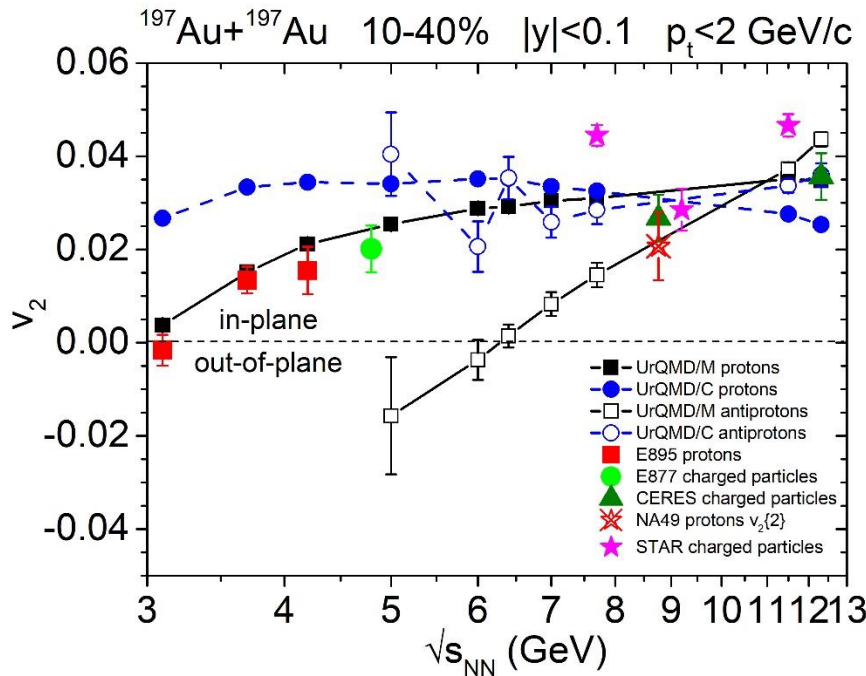




# Effects of EoS



# Effects of EoS



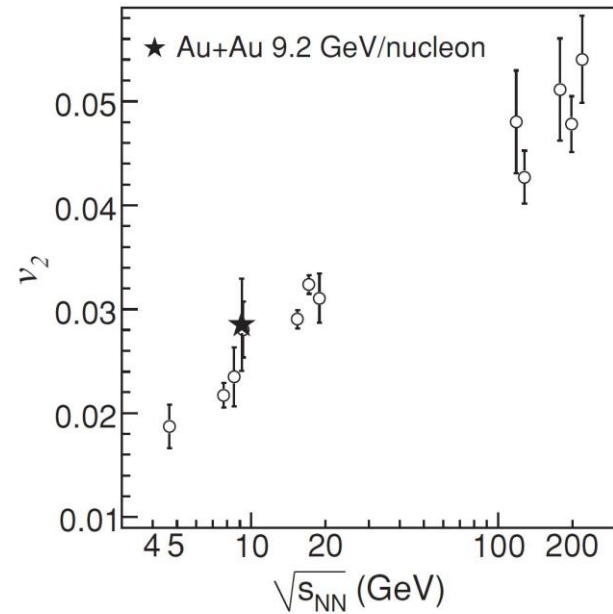
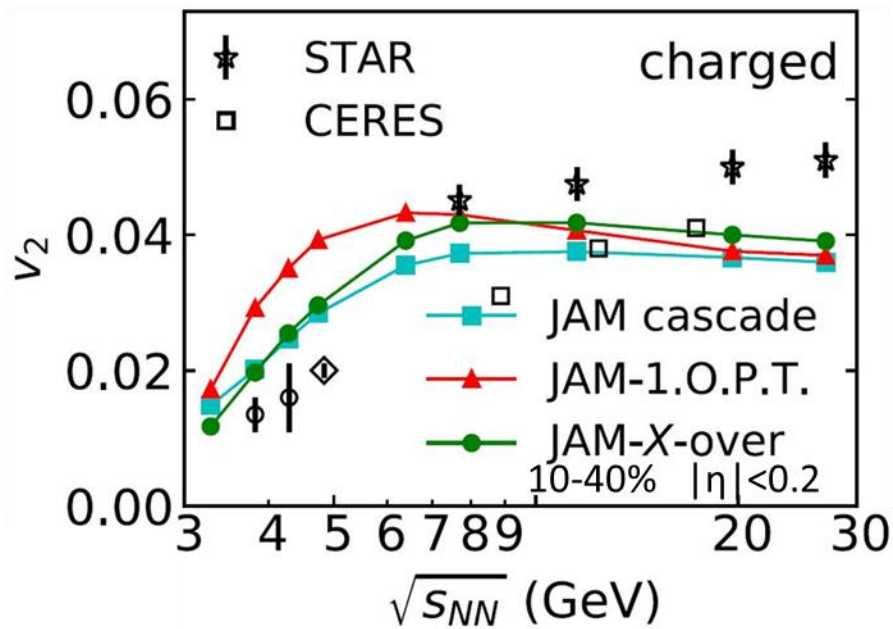
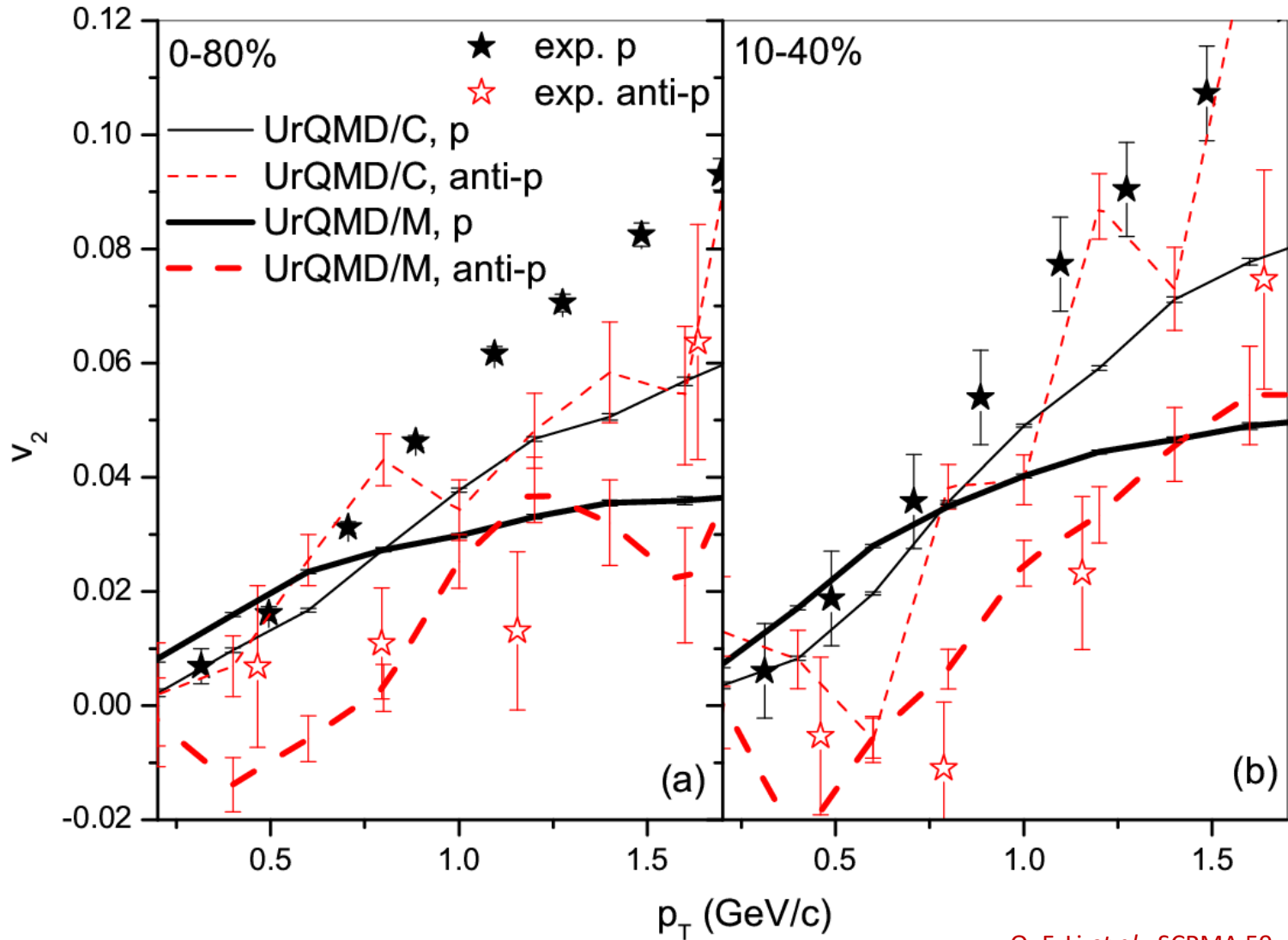


FIG. 24. Energy dependence of  $v_2$  near midrapidity ( $-1 < \eta < 1$ ) for  $\sqrt{s_{NN}} = 9.2$  GeV 0–60% central Au+Au collisions. Only statistical errors are shown. The results of STAR charged-hadron  $v_2$  [55] are compared with those measured by E877 [56], NA49 [54], PHENIX [57], and PHOBOS [46,50,58] collaborations.

$^{197}\text{Au} + ^{197}\text{Au}; s_{\text{NN}}^{1/2} = 7.7 \text{ GeV}; |\eta| < 1$



Q. F. Li *et al.*, SCPMA 59, 632001 (2016)

Effects of hadronic mean-field potentials on  $v_2$  splitting

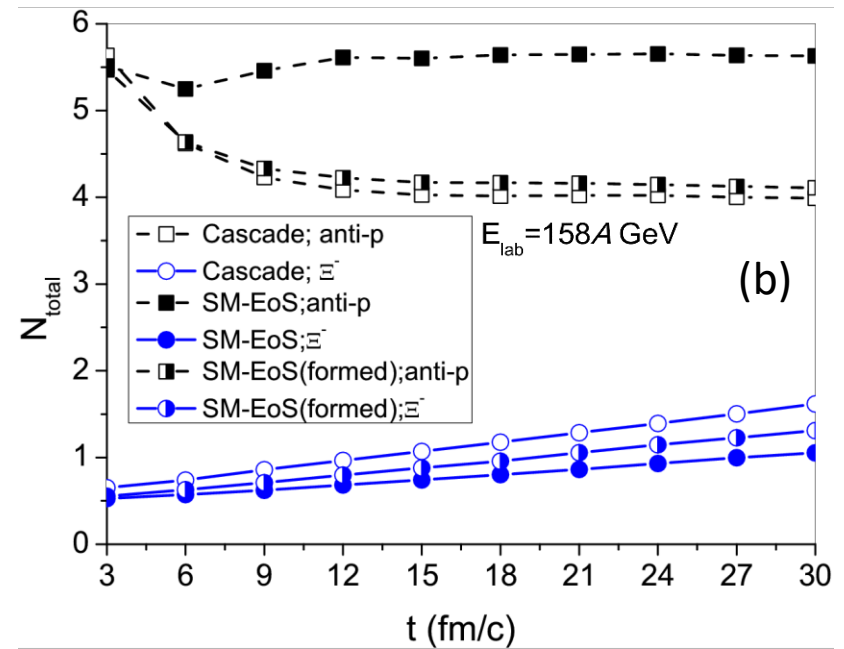
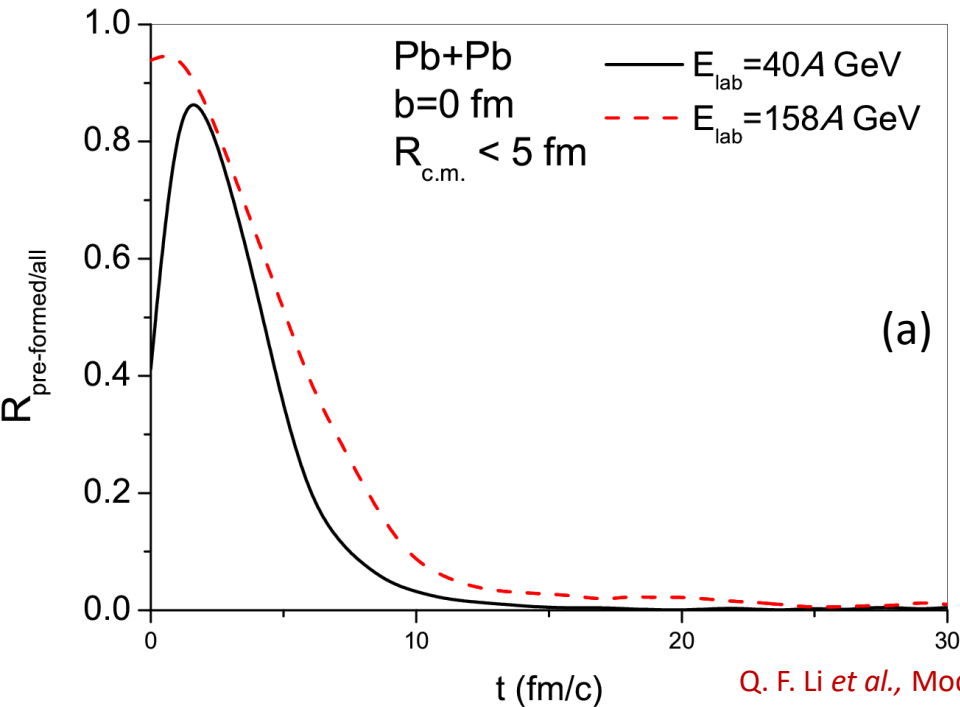
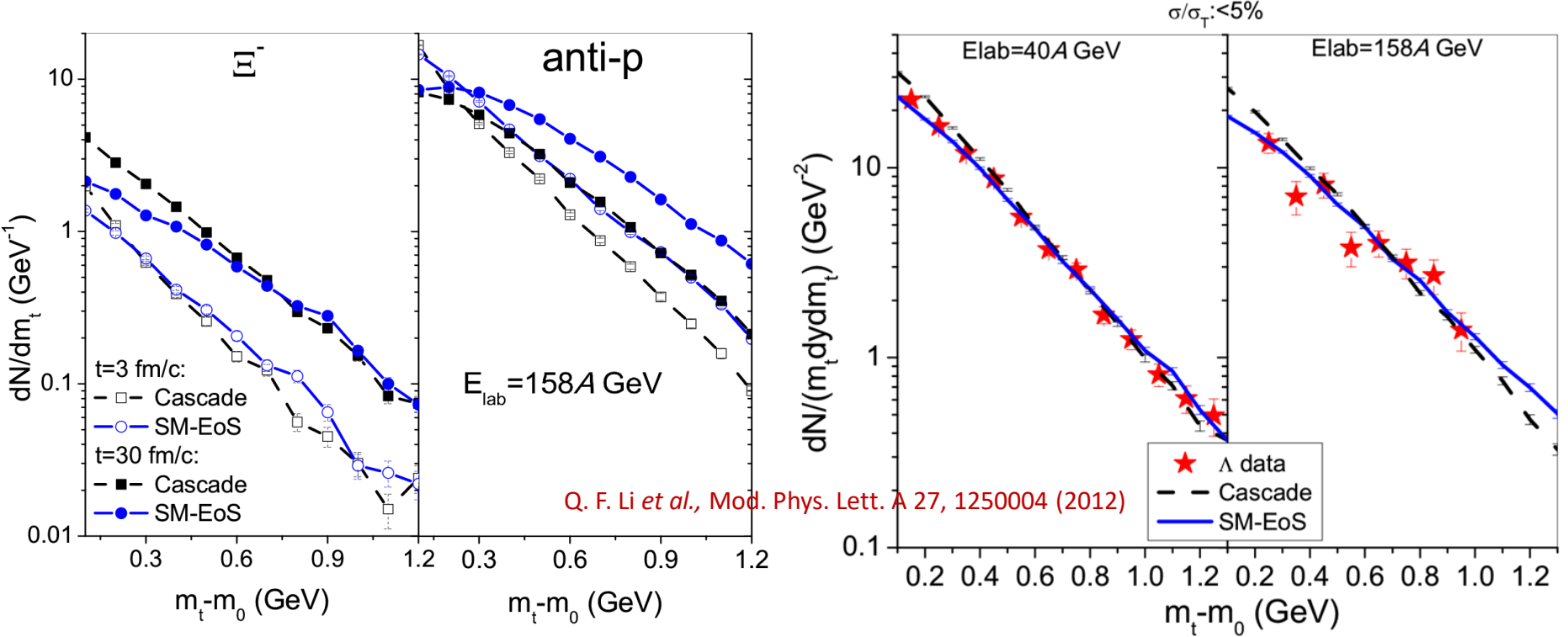


Fig.(a), the main production mechanism at  $t < 5$  fm/c is string excitation and fragmentation, and that this production mechanism still plays visible role up to  $t \sim 10$  fm/c. Hence, the pre-formed hadron potentials will definitely provide a visible contribution to the early pressure.

Fig.(b), if switch off the pre-formed hadron potentials but keep the formed ones, the time evolution of  $\bar{p}$  is almost the same as that with the cascade mode. Means that the mechanism of string excitation and fragmentation is essential to the production of  $\bar{p}$ .

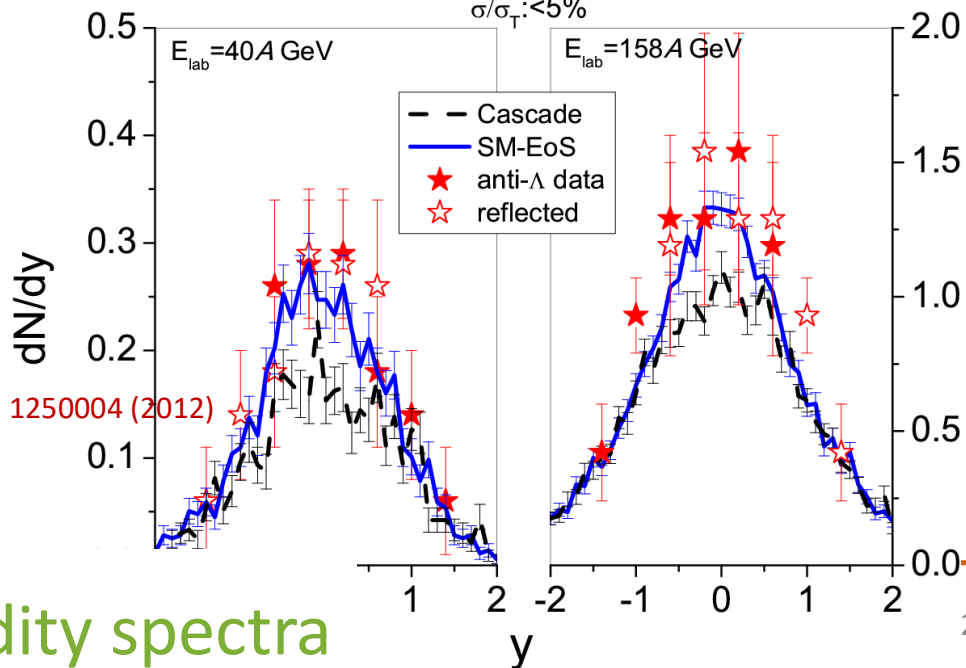
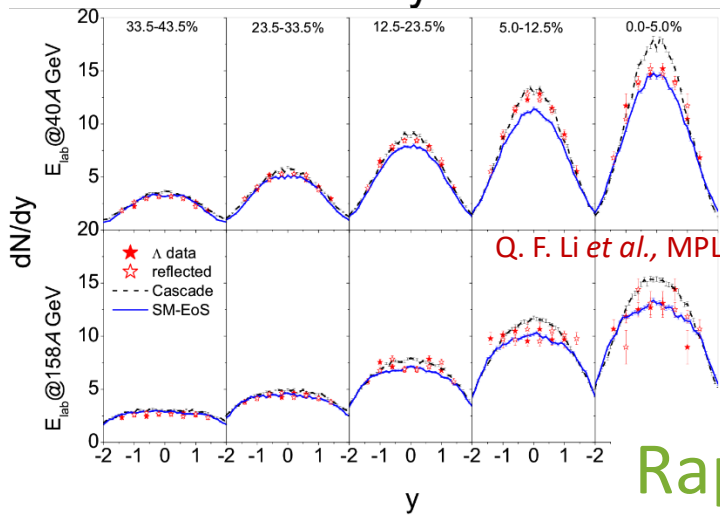
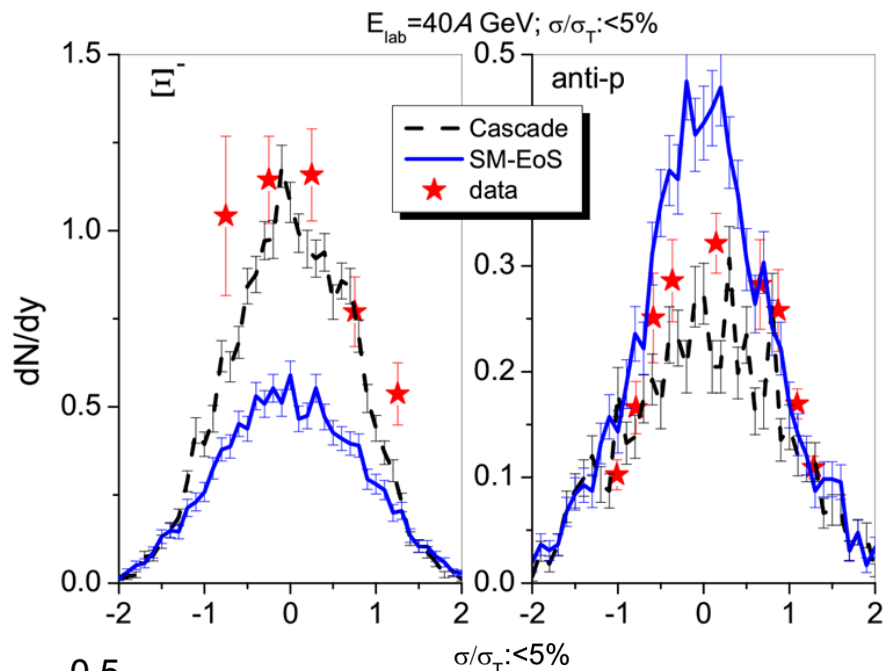
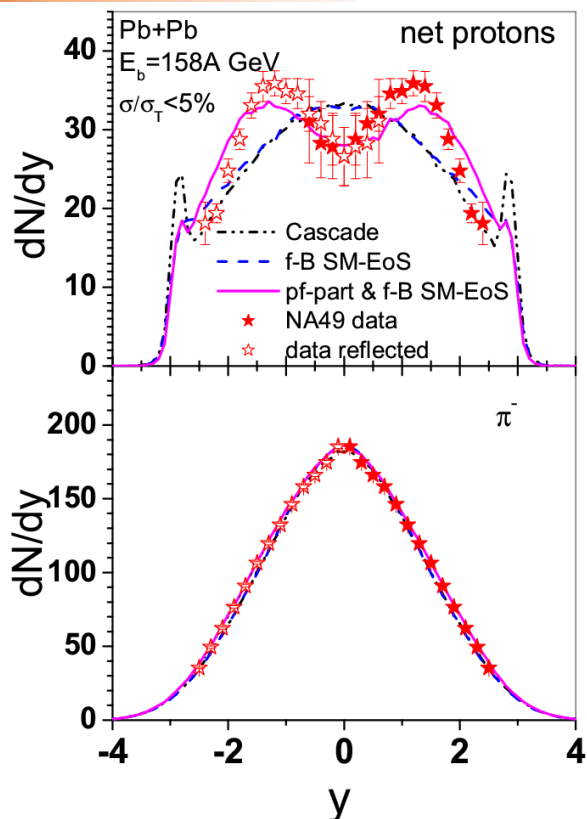


Q. F. Li *et al.*, *Mod. Phys. Lett. A* 27, 1250004 (2012)

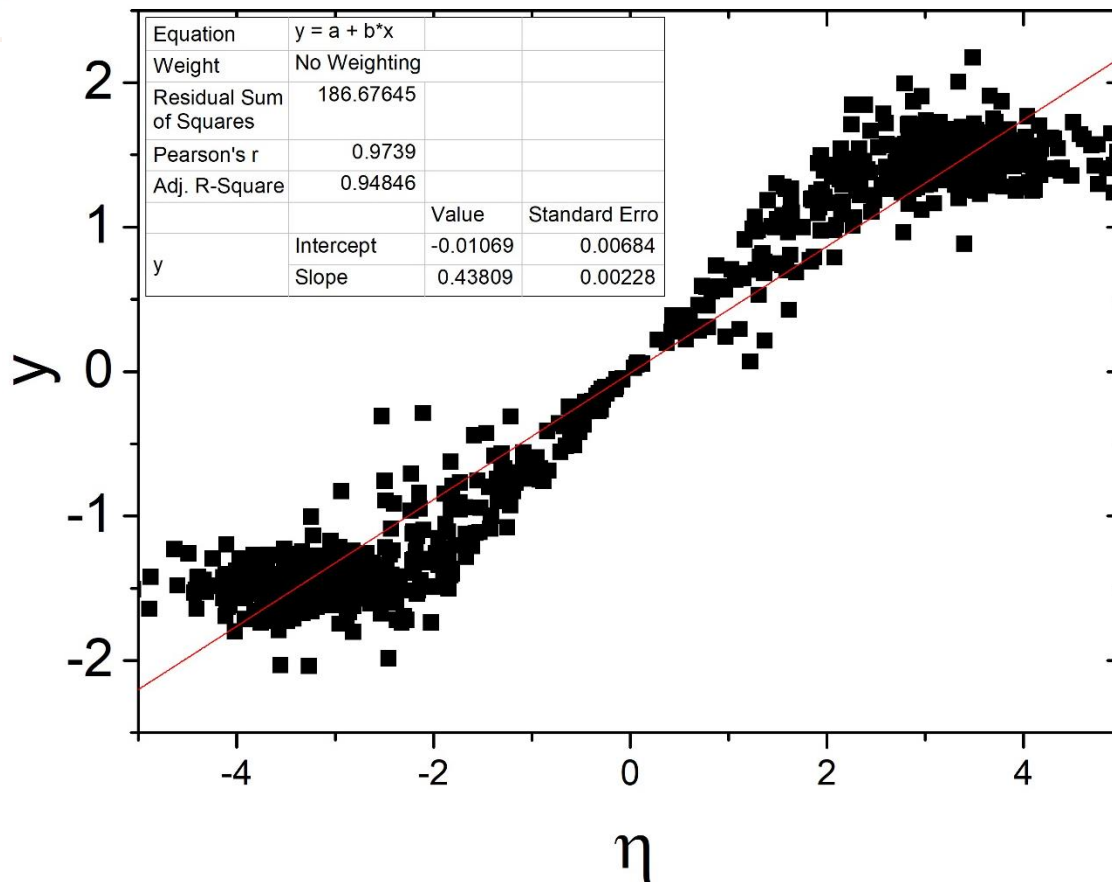
For strange particle production, in addition to the string mechanism, the rescattering process of hadrons are also important:

- (i) the rapid increase of the  $\Xi^-$  yield during the time 3~30 fm/c,
- (ii) the suppression effect of potentials on both the yield mainly at the low transverse masses and the total yield at  $t = 30$  fm/c,
- (iii) the contribution of formed hadron potentials to  $\Xi^-$  yield.

## Transverse mass spectra



Rapidity spectra



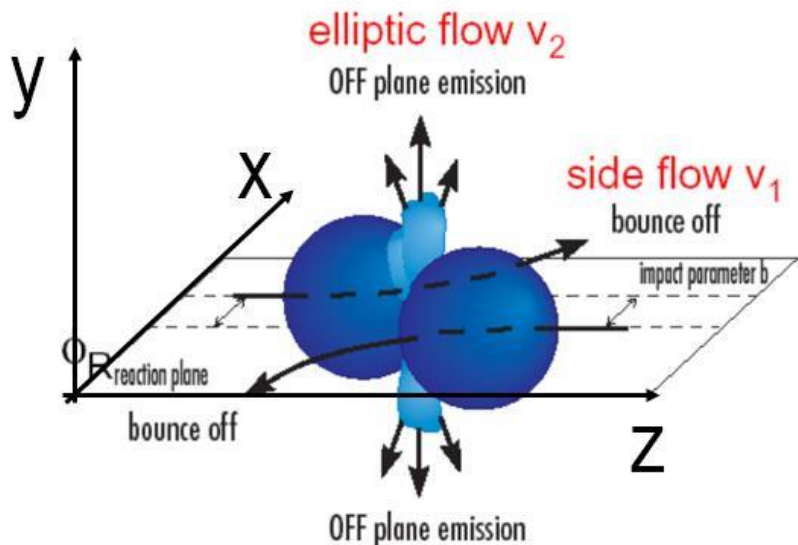
$y = \frac{1}{2} \ln \frac{E + p_{\parallel}}{E - p_{\parallel}} = \frac{1}{2} \ln \frac{1 + v_{\parallel}}{1 - v_{\parallel}}$  来表示， $v_{\parallel} = \frac{p_{\parallel}}{E}$  是粒子的纵向速度

另外，当粒子的质量与纵向动量相比可以忽略时， $E = p$ ，由此可得。

$$y \approx \frac{1}{2} \ln \frac{1 + \cos \theta}{1 - \cos \theta} = -\ln \operatorname{tg} \frac{\theta}{2} = \eta,$$

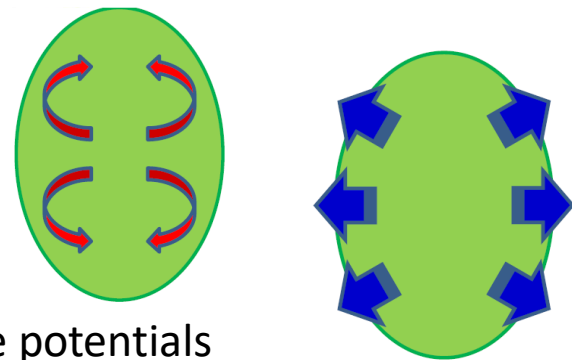
其中  $\theta$  是粒子动量与纵方向的夹角， $\eta$  是实验中常用的量，称为赝快度。32





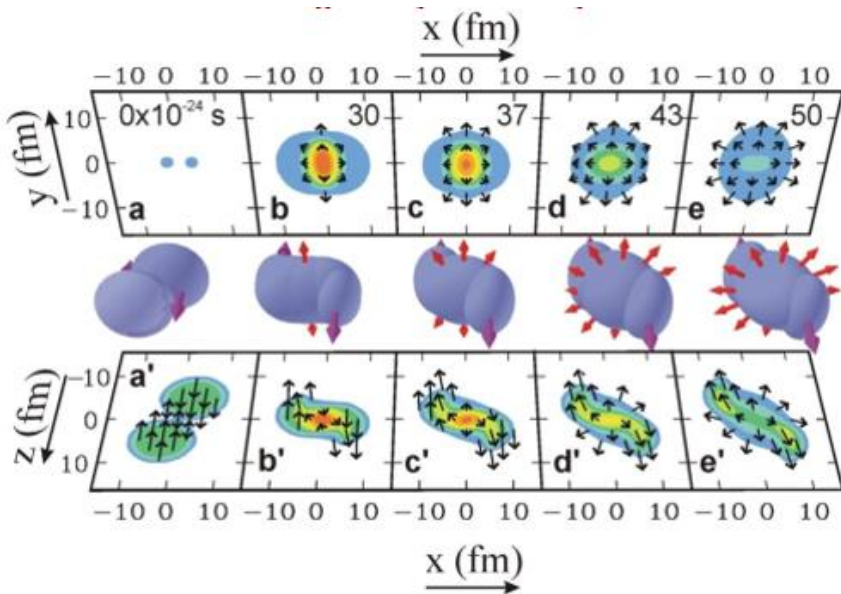
Particles with attractive potentials are more likely to be trapped in the system

$v_2$  decrease



Particles with repulsive potentials are more likely to leave the system

$v_2$  increase



P. Danielewicz *et al.*, Science (2002).

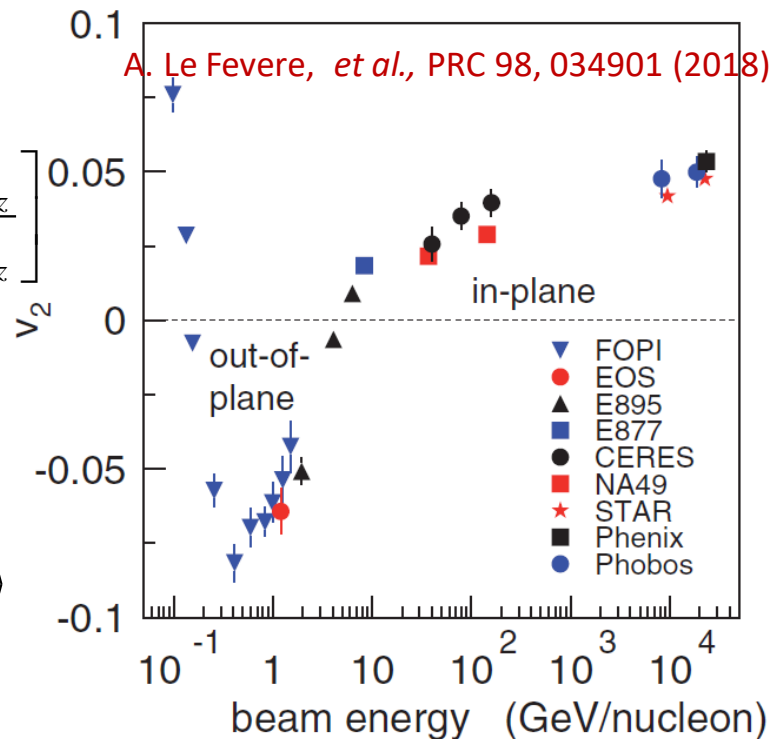
$$p_t = \sqrt{p_x^2 + p_y^2}$$

$$y = \frac{1}{2} \ln \left[ \frac{E + p_z}{E - p_z} \right]$$

$$v_1 = \left\langle \frac{p_x}{p_t} \right\rangle$$

$$v_2 = \left\langle \frac{p_x^2 - p_y^2}{p_t^2} \right\rangle$$

A. Le Fevère, *et al.*, PRC 98, 034901 (2018)





Different hadronic and partonic potentials for particles and antiparticles

J. Xu, L.W. Chen, C.M. Ko, Z.W. Lin, PRC 85, 041901(R) (2012); J. Xu, T. Song, C. M. Ko, F. Li, PRL 112, 012301 (2014)

the different mean-field potentials for hadrons and antihadrons or quarks and antiquarks:

## A multiphase transport (AMPT) model with string melting

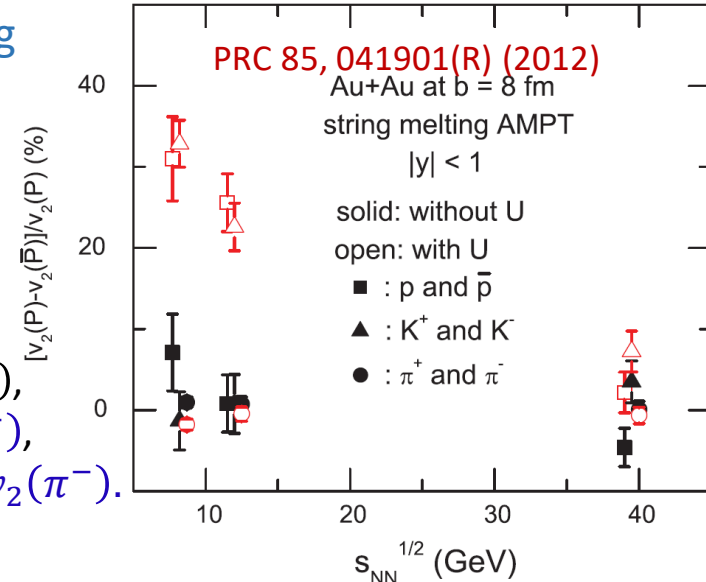
$$U_{N,\bar{N}}(\rho_B, \rho_{\bar{B}}) = \Sigma_s(\rho_B, \rho_{\bar{B}}) \pm \Sigma_v^0(\rho_B, \rho_{\bar{B}})$$

$\Sigma_s(\rho_B, \rho_{\bar{B}})$  nucleon scalar self-energies,

$\Sigma_v^0(\rho_B, \rho_{\bar{B}})$  nucleon vector self-energies

“+” for nucleons, “-” for antinucleons

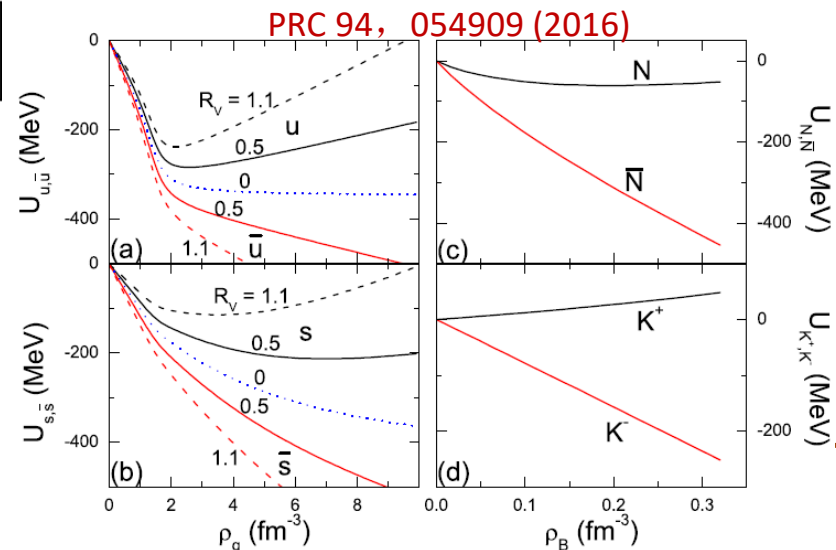
Stronger **attractive** potential for  $\bar{p}$  compared to  $p \rightarrow$  smaller  $v_2(p)$ ,  
**Attractive** potential for  $K^-$ , **repulsive** for  $K^+ \rightarrow v_2(K^-) < v_2(K^+)$ ,  
 Slightly **attractive** potential for  $\pi^+$ , **repulsive** for  $\pi^- \rightarrow v_2(\pi^+) < v_2(\pi^-)$ .



## 3-flavor Nambu-Jona-Lasinio transport model

$$\begin{aligned} \mathcal{L} = & \bar{\psi}(i \not{\partial} - M)\psi + \frac{G}{2} \sum_{a=0}^8 \left[ (\bar{\psi} \lambda^a \psi)^2 + (\bar{\psi} i \gamma_5 \lambda^a \psi)^2 \right] \\ & + \sum_{a=0}^8 \left[ \frac{G_V}{2} (\bar{\psi} \gamma_\mu \lambda^a \psi)^2 + \frac{G_A}{2} (\bar{\psi} \gamma_\mu \gamma_5 \lambda^a \psi)^2 \right] \\ & - K \left[ \det_f \left( \bar{\psi} (1 + \gamma_5) \psi \right) + \det_f \left( \bar{\psi} (1 - \gamma_5) \psi \right) \right], \end{aligned}$$

With a nonvanishing  $G_V$ , it further gives rise to a **repulsive** vector mean-field potential for quarks but an **attractive** one for antiquarks in a baryon-rich quark matter.



The difference of  $v_2$  between transported quarks and produced quarks during the initial stage of HICs. *J. C. Dunlop, et al., PRC 84, 044914 (2011).*

Baryon stopping effect and scattering. (By tracing the number of initial quarks in protons in the UrQMD).

*B. Tu, et al., CPC 43, 054106 (2019).*

1. Produced protons (0 iq) and antiprotons: **made of produced quarks, produced in the early stage**, experience the full evolution of the system, **experience similar magnitude of interactions.**

$$\rightarrow v_2(p(0\text{ iq})) \approx v_2(\bar{p})$$

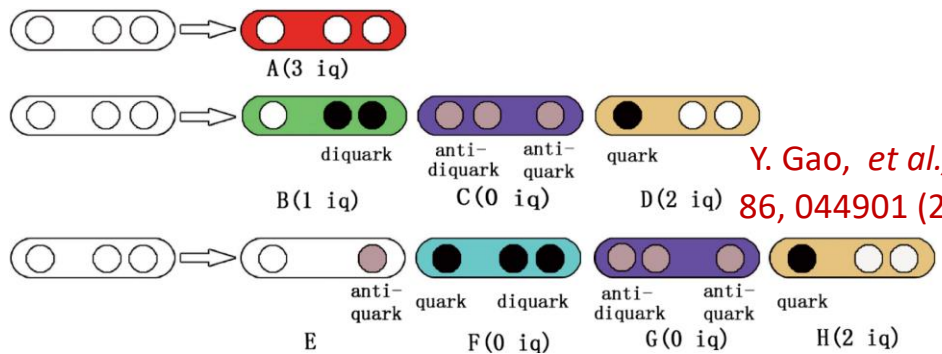
2.  $v_2$  of transported protons (3 iq) derives from the transport **from forward rapidity to mid-rapidity** due to the **nuclear stopping effect.**

$$\rightarrow v_2(p(3\text{ iq})) > v_2(p(0\text{ iq})) \approx v_2(\bar{p})$$

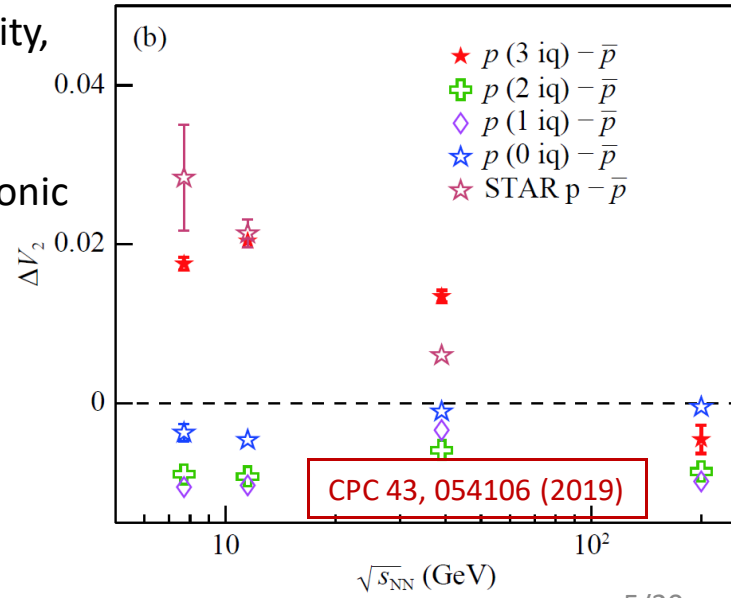
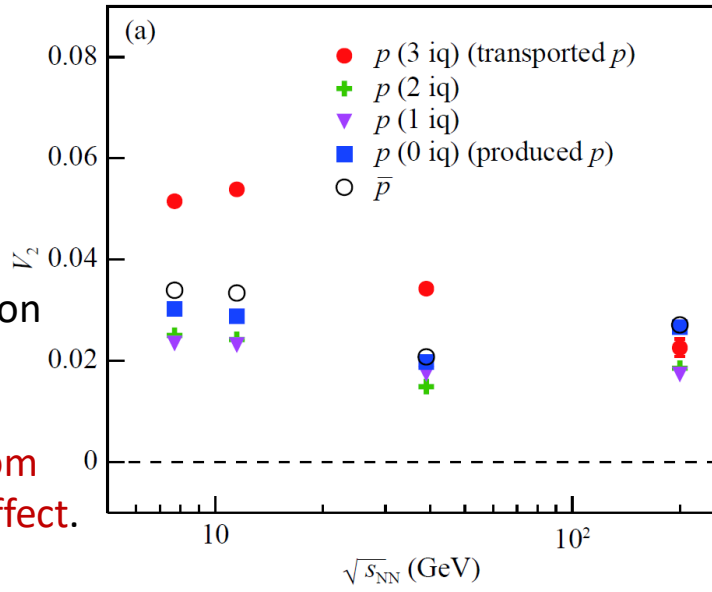
3. Transported quarks, which are transported over a large rapidity, **suffer more scatterings** than produced quarks.

$$\rightarrow v_2(p(3\text{ iq})) > v_2(p(0\text{ iq}))$$

4. Large deviation at high energies  $\geq 39$  GeV suggests that hadronic interactions are dominant in collisions at 7.7 and 11.5 GeV.

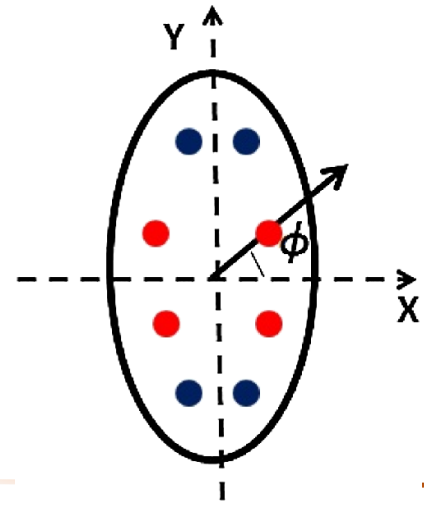
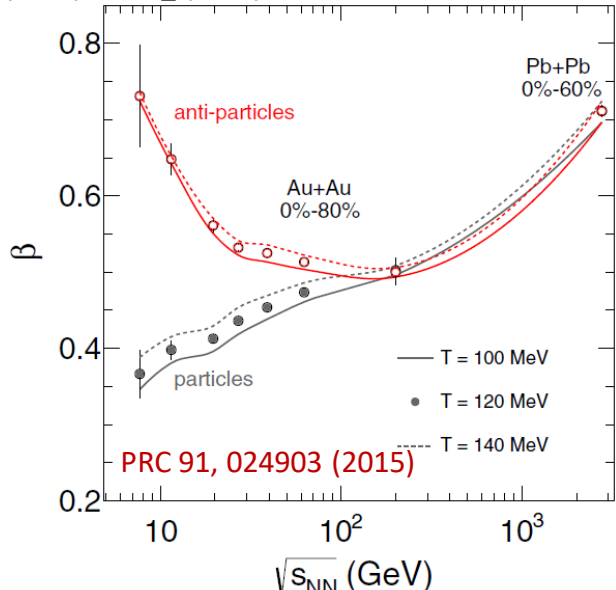
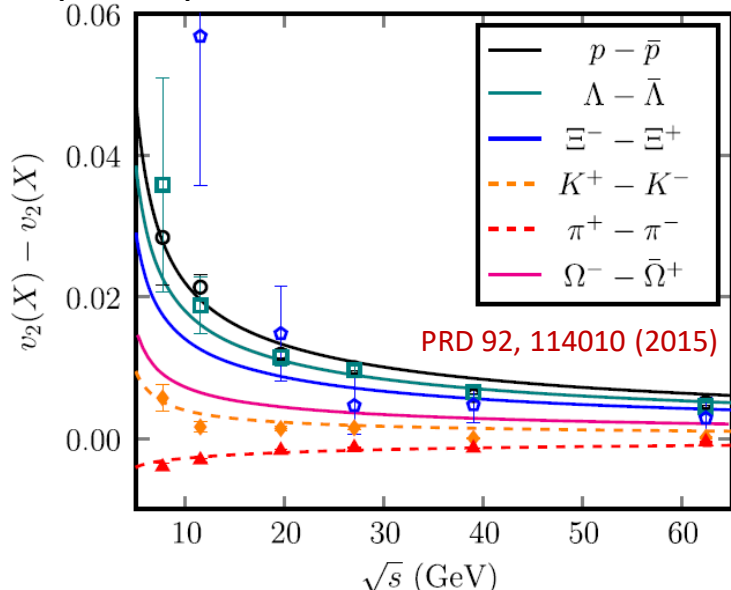
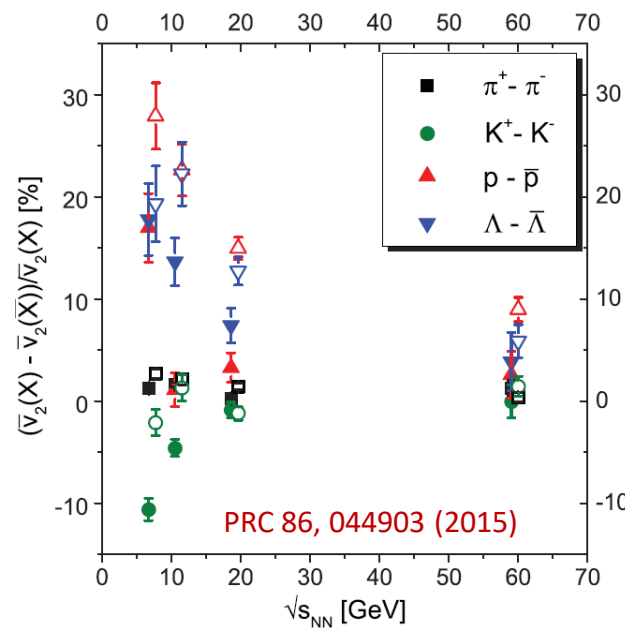


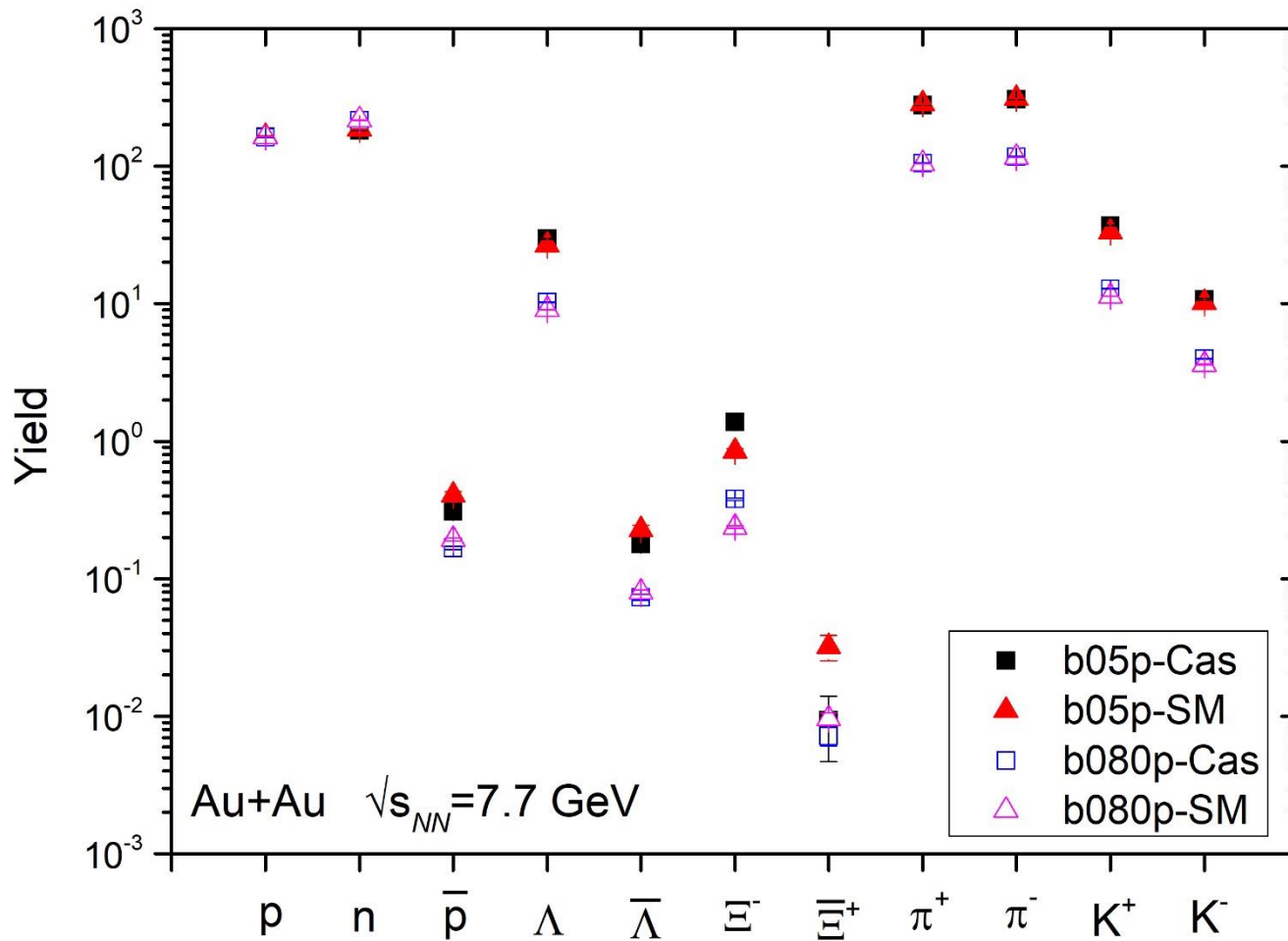
*Y. Gao, et al., PRC 86, 044901 (2012).*



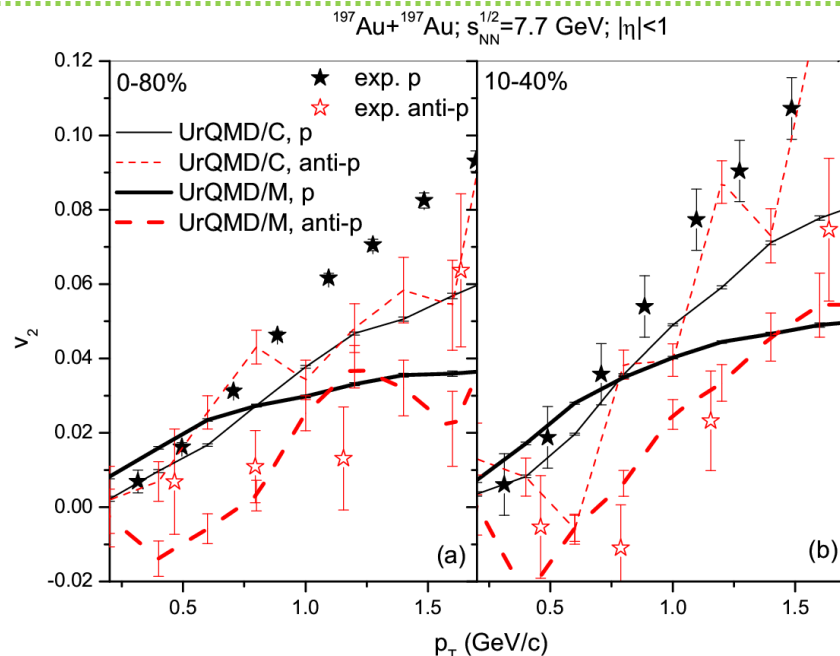
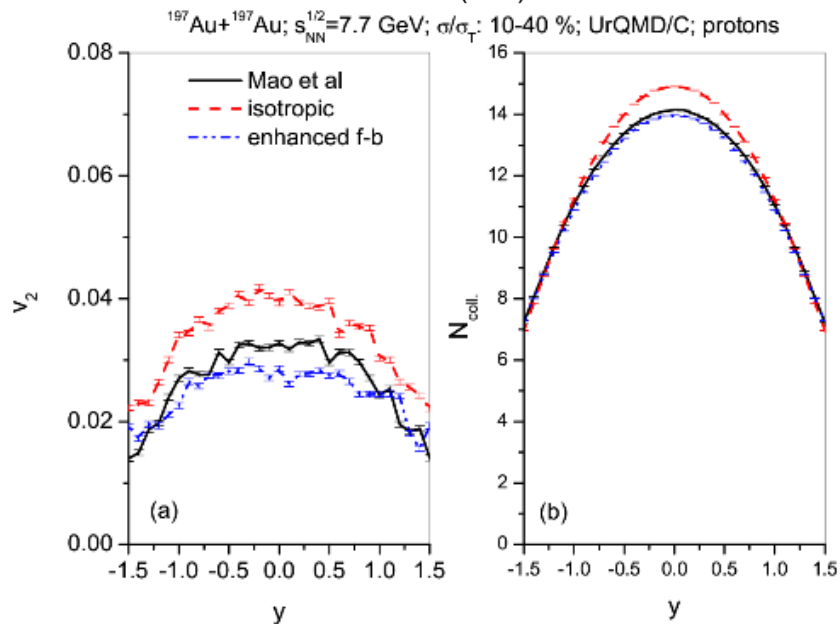
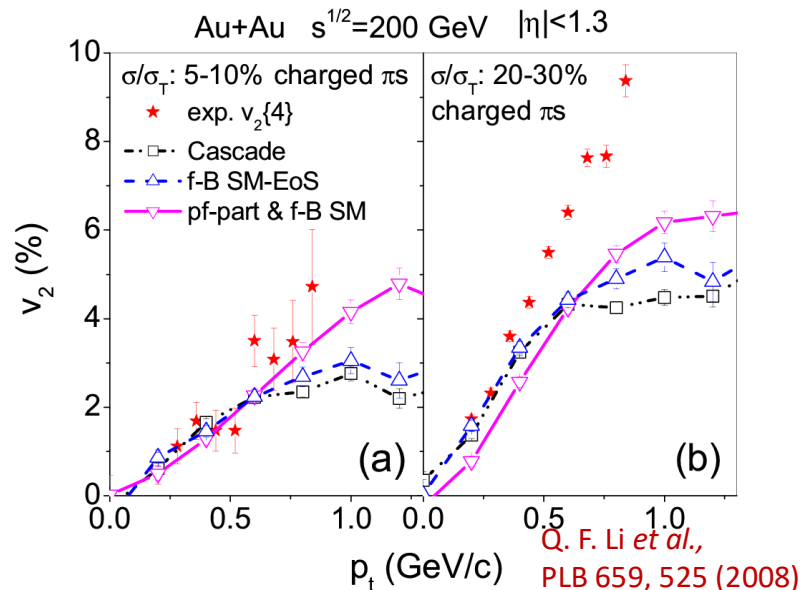
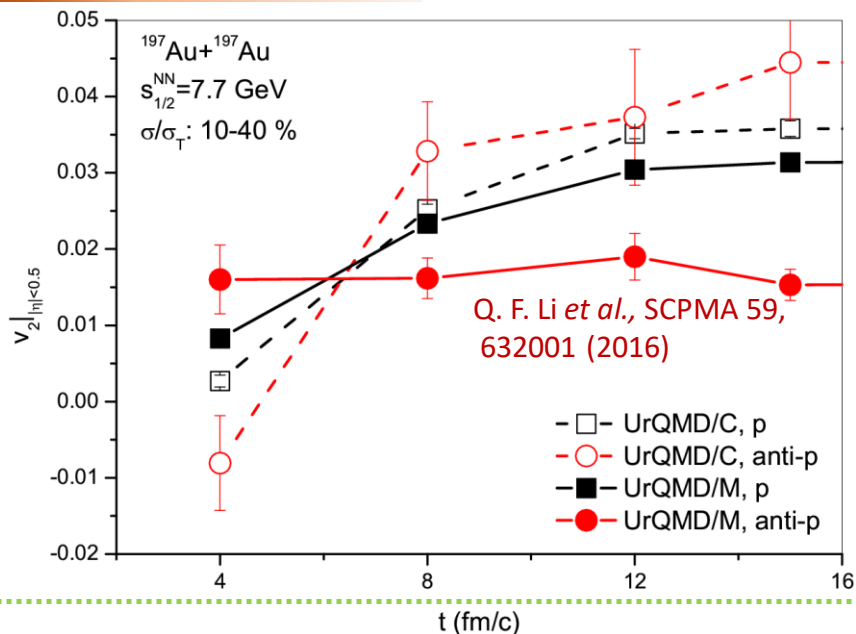
Particle production in a string-excitation scheme in UrQMD.

- By variations in the widths of quark and antiquark rapidity distribution. *V. Greco, et al., PRC 86, 044905 (2012).*
- Conservation of baryon charge, strangeness, and isospin. *J. Steinheimer, et al., PRC 86, 044903 (2012)*
- Hydrodynamics at finite baryon chemical potential. *Y. Hatta, et al., PRD 92, 114010 (2015).*
- Energy dependent difference of the transverse expansion velocity  $\beta$  between particles and corresponding antiparticles. *X. Sun, et al., PRC 91, 024903 (2015).*
- The strong magnetic field in noncentral collisions  $\rightarrow$  Chiral magnetic wave  $\rightarrow$  the electric quadrupole moment of the QGP  $\rightarrow v_2(\pi^+) < v_2(\pi^-)$ . *Y. Burnier, et al., PRL 107, 052303 (2011).*





# Results from UrQMD: $v_2$ difference



Effects of hadronic mean-field potentials on  $v_2$  splitting